



MINISTRY OF TECHNOLOGY

AERONAUTICAL RESEARCH COUNCIL  
REPORTS AND MEMORANDA

# The Response of a Constant-Pressure Turbulent Boundary Layer to the Sudden Application of an Adverse Pressure Gradient

By P. Bradshaw

LIBRARY  
ROYAL AERONAUTICAL ESTABLISHMENT  
BEDFORD.

LONDON: HER MAJESTY'S STATIONERY OFFICE

1969

PRICE 15s. 0d. NET

# The Response of a Constant-Pressure Turbulent Boundary Layer to the Sudden Application of an Adverse Pressure Gradient

By P. Bradshaw

---

*Reports and Memoranda No. 3575\**

*January, 1967*

---

## *Summary.*

Mean velocity, turbulent intensity and shear stress have been measured in a turbulent boundary layer which passes from a region of constant free-stream velocity  $U_1$  to a region with  $U_1 \propto x^{-0.255}$ . Further measurements and calculations have been made for a range of initial boundary-layer thicknesses.

---

## CONTENTS

### *Section.*

1. Introduction
2. Apparatus and Procedure
3. The Mean Velocity Profiles and Surface Shear Stress
4. The Shear Stress and Intensity Profiles in Layer 'C'
5. The Eddy-Viscosity and Mixing-Length Distributions
6. The Energy Balance for Layer 'C'
7. Calculations of Development with Different Initial Conditions
8. Conclusions

List of Symbols

References

Table 1

Illustrations—Figs. 1 to 16

Detachable Abstract Cards

---

\*Replaces NPL Aero Report 1219—A.R.C. 28 663.

## 1. Introduction.

In Ref. 1, a description was given of the response of an equilibrium boundary layer, which had developed in a region where the free-stream velocity varied as  $x^{-0.255}$ , to the sudden removal of pressure gradient. In the present Report, a description is given of a boundary layer which initially develops in zero pressure gradient and then passes into a region where the free-stream velocity varies as  $(x-x_1)^{-0.255}$ . There is no quantitative connection or antithesis between the behaviour of the two boundary layers, and  $-0.255$  was chosen as the exponent in the boundary layer described below solely in order that the asymptotic state of the boundary layer far downstream should be known from previous measurements. The equilibrium boundary layer itself is described in Refs. 1 and 2.

A boundary layer which tends slowly towards a second equilibrium state instead of separating should, like the boundary layer of Ref. 1, be a good test of methods of calculating turbulent boundary layers: in both cases the effects of the 'mis-match' between the old boundary layer and the new pressure distribution gradually die away. The boundary layer of Ref. 1 was a rather severe and unusual case but that described in the present Report is more like the boundary layer on a typical 'roof top' aerofoil, and the results are therefore of more practical interest. The measurements have, in fact, thrown some light on the surprisingly good performance of mixing-length and 'local-equilibrium' methods of calculation in non-equilibrium retarded boundary layers. That the results contain no spectacular features is merely an indication that we now have reasonably firm ideas of how this sort of boundary layer ought to behave, and that further experimental work should be concentrated on investigation of turbulence processes rather than overall flow development.

As well as the experimental results, some examples are given of calculations of the boundary-layer development, by the method of Ref. 3, for a larger range of  $x_1$  than is covered by the experiments. The method is believed to be sufficiently accurate for the results to be a useful extension of the wind-tunnel measurements, at least for the purposes of a qualitative discussion.

The relevance of the experimental results to the production of drag increments due to thickening of the boundary layer by roughness elements has been discussed in Ref. 4.

Since this work was done, we have seen the thesis of Goldberg<sup>5</sup> which describes measurements (in the same tunnel as Moses<sup>6</sup>) of mean velocity,  $u$ -component intensity and shear stress in a total of five pressure distributions which may be regarded as exaggerated versions of those of Ref. 1 and the present experiment. The variations of eddy viscosity and mixing length are larger than in the latter experiments (note that Goldberg makes the mixing length dimensionless by dividing by the displacement thickness rather than the total thickness of the boundary layer) but the really large variations only occur very near separation, when shear-stress gradients in the outer part of the flow are much smaller than the pressure gradient and therefore need not be represented very accurately.

## 2. Apparatus and Procedure.

The measurements were made in the NPL 59 in. x 9 in. (1.5m x 0.23m) boundary-layer tunnel<sup>7</sup> at a reference speed of 120 ft/sec (37 m/s) and with the surface pressure distribution shown in Fig. 1. Turbulence measurements were made with constant-temperature linearized hot-wire anemometers, the apparatus and techniques being generally similar to those described in Ref. 8. The measurements were made in winter, when the air in Teddington is dirty and the power supply voltage unsteady, and are more scattered than those of Ref. 1.

The thinnest of the three boundary layers, (boundary layer 'A'), was tripped by a spanwise wire about an inch behind the leading edge. Boundary layer 'B' was artificially thickened by sandpaper extending from the leading edge to  $x = 11$  in., and boundary-layer 'C' was thickened by the same arrangement of sandpaper and by obstacles at the leading edge: the obstacles were cable clips about 1/4 in. high mounted 1/2 in. apart. The total thicknesses (to  $U/U_1 = 0.955$ ) of the three boundary layers at  $x = 24$  in., where the measurements started, were 0.47 in., 0.69 in. and 1.12 in. respectively. Boundary layers B and C were not quite the same as equilibrium boundary layers in zero pressure gradient at the same Reynolds number but this is of no importance for the present discussion. These artificially-thickened layers showed no evidence of any abnormalities in turbulence structure: for instance, the surface shear stress at  $x = 24$  in.

agreed accurately enough with the various formulae  $c_f = f(H, U_1 \delta_2/v)$  and the further development of layers A and C was adequately predicted by the calculation method of Ref. 3, which assumes universal relations between the shear stress and the turbulence structure.

Unfortunately, the sandpaper used to thicken the boundary layer tore loose after the completion of the mean-velocity and intensity measurements in layer C – the glue used to attach it to the surface was subsequently found to be adulterated – so that the shear-stress measurements, made after replacing the sandpaper and leading-edge excrescences, refer to a slightly different boundary layer. The checks made at the time showed the discrepancies to be small but, in fact, the second boundary layer was slightly thinner, so that the measured ratio of shear stress to turbulent intensity is too small near the edge of the boundary layer where both quantities decrease very rapidly with increasing  $y$ .

The boundary layers remained so nearly two-dimensional that calculations of the virtual origin of lateral convergence<sup>1</sup>,  $x = x_0$ , from the out-of-balance term in the momentum integral equation,  $\delta_2/(x - x_0)$ , gave scattered positive and negative values: convergence has therefore been neglected in the analysis of the results.

### 3. The Mean Velocity Profiles and Surface Shear Stress.

The mean velocity profiles in layers 'A', 'B' and 'C' are shown in Fig. 2. The profile parameters and surface shear stress (the latter measured with a Preston tube using Head and Rechenberg's<sup>9</sup> calibration) are shown in Figs. 3 to 7 and tabulated in Table 1. The approximate figures for  $c_f$  and  $H$  in the equilibrium boundary layer with  $U_1 \alpha x^{-0.255}$  at a representative Reynolds number are given at ' $x = \infty$ '. The boundary layers appear to be tending monotonically to the equilibrium state but a great distance would be required for equilibrium to be attained. The profile shape parameter  $H$  varies only slightly: even in the equilibrium boundary layer it is only about 1.55 in this range of Reynolds number. Values of  $H$  exceeding 2 are found only close to separation (see Section 7): in moderately retarded boundary layers the variation of  $H$  with Reynolds number is almost as important as the variation due to pressure gradient. The pressure gradient in these boundary layers is by no means small:  $(\delta_1/\tau_w) dp/dx$ , which is the ratio of the pressure-gradient term in the momentum integral equation to the surface shear-stress term since  $\frac{d}{dx} (\rho U_1^2 \delta_2) = \tau_w + \delta_1 \frac{dp}{dx}$ , reaches 3 in layer 'C' compared with 5.4 in the equilibrium boundary layer, and the surface shear-stress coefficient falls to as little as 0.7 of the value in zero pressure gradient at the same Reynolds number, compared with about 0.55 in the equilibrium boundary layer. The pressure rise to  $x = 84$  in. is about 0.46 of the initial dynamic pressure.

### 4. The Shear Stress and Intensity Profiles in Layer 'C'.

The response of the boundary layer to the sudden application of an adverse pressure gradient is of course a more rapid decrease in  $U/U_1$  along any streamline within the boundary layer. If the pressure gradient is strong the retardation in the outer layer can be predicted in the early stages by assuming that the shear stress on a given streamline remains unchanged, as demonstrated, for instance, in Ref. 10.

An explanation of the slow reponse of the shear stress to changes in pressure gradient was given in Ref. 1: briefly, if  $dp/dx$  increases suddenly,  $\partial U/\partial y$  and the turbulence production increase linearly and the turbulent intensity and shear stress increase parabolically. Near the wall, the time scale of the turbulence (the ratio of the intensity to the production rate, say) is so small that adjustment takes place very quickly, and the inner layer is an 'equilibrium layer' in the sense of Ref. 8. In the present boundary layer, the application of pressure gradient is fairly mild and the response of the shear stress is not so clear-cut as in the ideal case discussed above: although  $\tau/\rho U_1^2$  increases with  $x$  in the central portion of layer 'C' (Fig. 8), the absolute shear stress decreases very slightly. At  $x = 84$  in.,  $\tau_{\max}/\tau_w \approx 2.4$  and  $\tau_{\max}/\rho U_1^2 = 0.002$ , compared with about 5 and 0.003 in the equilibrium boundary layer, so that the boundary layer is still far from equilibrium even though  $H$ , at 1.54, is almost exactly the same as the equilibrium value.

The intensity profiles (Fig. 9) show the same trends as the shear stress profile: it is noticeable that

near the wall  $\tau/\rho \overline{q^2}$  decreases with increasing  $x$  as the 'inactive' motion,<sup>11,12</sup> imposed on the flow near the wall by the larger-scale turbulence in the central part of the layer, increases in strength compared with the local, shear-stress-producing, 'active' motion. A better impression of rates of change in the streamwise direction is given by the advection (Fig. 12(c)).

##### 5. The Eddy-Viscosity and Mixing-Length Distributions.

The mixing length formula can be re-written

$$\tau/\rho \frac{\partial U}{\partial y} = \frac{(\tau/\rho)^{3/2}}{l}$$

The term on the left is the production rate: the term on the right is similar to the form  $(\tau/\rho)^{3/2}/L$  used to represent the dissipation by Townsend<sup>11</sup> and Bradshaw *et al.*<sup>3</sup> Townsend pointed out that, in the inner layer, local-similarity conditions required both that  $L \propto y$  and that (production) = (dissipation), at least in small shear-stress gradients: thus  $L$  was equated to  $l$ . Bradshaw *et al.* showed empirically that  $L/\delta$  was a universal function of  $y/\delta$  throughout the boundary layer, an average value outside the inner layer being about 0.08: thus  $L$  and  $l$  are again equal if (production) = (dissipation). In equilibrium boundary layers (constant  $(\delta_1/(\tau_w)dp/dx)$ ), production and dissipation *are* nearly equal because diffusion happens roughly to balance advection in the outer layer, and  $l$  is found experimentally to be nearly  $0.08\delta$  for all equilibrium boundary layers<sup>2</sup>. In the boundary layer of Ref. 1, however, the advection becomes very large and negative as the turbulence decays, and the mixing length rises considerably.

For the reasons mentioned in Section 2, the experimental values of mixing length decrease slightly near the outer edge of the present boundary layer 'C' instead of rising rapidly to infinity (Fig. 10), but the values in the central part of the layer are reliable enough. The mixing length at  $x = 24$  in. has the expected value of about  $0.08 \delta_{99.5}$  in the outer 80 per cent of the layer. On application of the adverse pressure gradient the average velocity gradient  $\partial U/\partial y$  over the outer part of the boundary layer starts to increase at once, but the shear stress responds more slowly because, as mentioned above, the *rate of change* of shear stress depends on the turbulence production  $\tau \partial U/\partial y$ : therefore, the dimensionless mixing length  $(\tau/\rho)^{1/2}/(\partial U/\partial y) \delta_{99.5}$  decreases downstream, and starts to increase again only just before the last station,  $x = 84$  in. The variation is much less spectacular than in the boundary layer of Ref. 1.

The decrease in mixing length must be allied with an increase in advection and in loss by diffusion. In fact, the advection in the part of the boundary layer near the shear-stress maximum is *negative* (and very small) because the absolute turbulent intensity  $\overline{q^2}$  decreases slowly along a streamline downstream although  $\overline{q^2}/U_1^2$  rises: the disparity between production and dissipation results chiefly in diffusion away from the shear-stress maximum and towards the outer edge of the growing boundary layer. The absolute value of the intensity integral  $\int \frac{1}{2} \overline{q^2} dy$  rises by a factor of about 1.9 between  $x = 24$  and  $x = 84$ , a factor not much greater than if the boundary layer had continued in zero pressure gradient, and the integrated advection  $\frac{d}{dx} \int U \frac{1}{2} \overline{q^2} dy$  is everywhere about 20 per cent of the integrated production for  $y/\delta > 0.2$ , compared with about 13 per cent in zero pressure gradient and 15 per cent in the equilibrium boundary layer with  $U_1 \propto x^{-0.255}$ . Thus, the integral of production over the central and outer part of the boundary layer is not much different from the integral of dissipation. This shows that the present boundary layer is much less strongly perturbed than the boundary layer of Ref. 1 where the advection rose to 40 per cent of the production.

The ratio of advection to production is a good measure of perturbation strength: since it is also a measure of the inaccuracy of a 'universal' mixing length distribution it follows immediately that mixing length methods will be acceptable only for weakly-perturbed boundary layers. The above distinction between absolute intensity and intensity normalized by  $U_1^2$  shows why the assumption of 'universal' mixing length is a particularly good one for boundary layers entering a region of mild adverse pressure

gradient because the advection is small (of the same order as in retarded equilibrium boundary layers). It is a particularly *bad* assumption in a boundary layer *leaving* a region of strong adverse pressure gradient because the advection is large and, moreover, of the opposite sign to the advection in retarded equilibrium boundary layers. It happened that the boundary layer of Ref. 1, which falls into this category, was explored only for the first fifteen boundary layer thicknesses after removal of the pressure gradient, so that although the dimensionless mixing length increased rapidly, it had only risen by about 15 – 20 per cent (30 – 40 per cent on shear stress) at the last measurement position, so that calculations assuming a constant mixing length gave quite good results in this restricted region.

The dimensionless eddy viscosity  $\nu_e/U_1 \delta_1$  (Fig. 11), which is again nearly the same in all equilibrium boundary layers, falls rapidly as soon as the pressure gradient is applied, and remains at less than two-thirds of the equilibrium value for the whole length of the flow. This variation of  $\nu_e/U_1 \delta_1 \equiv (\tau/\rho)/(\partial U/\partial y)$ .  $U_1 \delta_1$  is about twice that of  $l/\delta_{99.5} \equiv (\tau/\rho)^{1/2}/(\partial U/\partial y)$ .  $\delta_{99.5}$ , as would be expected from the dependence of these two quantities on shear stress, although the increase in  $\delta_1/\delta_{99.5}$  contributes to the variation. Changing the definition of dimensionless eddy viscosity to  $\nu_e/U_1 \delta_{99.5}$  would mean discarding the useful – if coincidental – constancy of  $\nu_e/U_1 \delta_1$  in equilibrium boundary layers, and my personal opinion is that mixing length is to be preferred to eddy viscosity because for data-correlation purposes it can be referred to the physically-meaningful dissipation length parameter.

In the inner layer of boundary layer ‘C’, the mixing length tends to about 0.4  $y$  as required by local equilibrium (equality of production and dissipation). One of the attractions of the mixing length approach is that it does at least give the right answer in the inner layer so that predictions of boundary layer development are never as ludicrously wrong in peculiar cases as are the predictions of the wholly-empirical methods. It would be possible to improve the assumption of a universal mixing length distribution by making some empirical allowance for advection, but this comes so near to the method of Ref. 3 (which allows for diffusion as well) that the latter is probably to be preferred.

#### 6. The Energy Balance for Layer ‘C’.

Most of the above discussion of results centres on the energy balance, and the various terms made dimensionless with  $U_{ref}$  and  $\delta_{99.5}$  are plotted for reference in Fig. 12. The advection and production were measured directly, while the dissipation was estimated by assuming that the dissipation length parameter  $L \equiv (\tau/\rho)^{3/1}/\epsilon$  was the same as that used in the calculation method of Ref. 3, which accurately predicts the development of this boundary layer: the diffusion was obtained by difference and its failure to integrate to zero across the layer is a measure of the experimental error and the inaccuracy of the assumption about  $L$ . Since  $\tau_{max}/\rho U_1^2$  increases only slowly with  $x$  the dimensionless diffusion near the edge of the boundary layer (which was shown in Ref. 3 to be directly related to the entrainment rate and roughly proportional to  $\tau_{max}/\rho U_1^2$ ) also increases rather slowly: the large (negative) values at  $x = 84$  in. result directly from the excessively large (positive) advection values, which can be blamed on the inevitable inaccuracy of graphical differentiation at the end of a range.

The considerable changes in the production profile sum up as well as anything the effect of pressure gradient on the boundary layer as a whole. The approximate constancy of the production in the outer half of the boundary layer is just a consequence of the scales used and has no particular physical significance.

#### 7. Calculations of Development with Different Initial Conditions.

It was considered unprofitable to do experiments with an initial boundary layer thick enough to separate because of the difficulty of maintaining two-dimensional flow. However, we have done some *calculations*, by the method of Ref. 3, with increasing thicknesses of initial boundary layer, in the same pressure distribution as was used in the experiments. A wide selection of test cases, including boundary layers A and C, has shown that the method is sufficiently realistic for such calculations to be useful at least for qualitative discussions.

For convenience, the calculations were done with a constant Reynolds number based on initial boundary-layer thickness, and thus with identical velocity and shear-stress profiles, using measurements

in layer *A* at  $x = 24$  in. The nominal boundary-layer thicknesses were 0.6 in. (1.5 cm), the same as in layer *A*, 1.3 in. (3.3 cm), the same as in layer *C*, 2.6 in. (6.6 cm), 3 in. (7.6 cm) and 3.3 in. (8.65 cm). Separation first occurs when the boundary layer is initially five times as thick as *A* or slightly more than twice as thick as *C*. It is noteworthy that the distance to separation is as much as 140 in.: the pressure-rise coefficient is about 0.6 and  $H$  is roughly 2.5. One of the virtues of this calculation method is that it does not use arbitrary criteria for separation but it is interesting to note that the value of  $H$  at separation is in the range 2.4 to 2.6 often used as a criterion of separation.

The most striking feature of the calculations shown in Fig. 14 is that two of the boundary layers overshoot the equilibrium values of  $H$  and  $c_f$ , approach separation and then return towards equilibrium. This behaviour was not necessarily to be expected, since one's intuitive feeling about turbulent flows is that their response to perturbations is heavily damped and that they always seek to develop in a self-preserving (equilibrium) way if the boundary conditions permit. It is highly unlikely that the calculated results are spurious; very close to separation, where the logarithmic region of the mean velocity profile disappears altogether, the results will be inaccurate, but a comparison of the theoretical profiles with Mellor's<sup>13</sup> slightly more refined theory suggests that errors are small for  $(\nu/u_\tau^3)\partial\tau/\partial y < 1$ , whereas the greatest value of this parameter reached in the 'overshooting' boundary layers is only 0.06. Clearly, it is possible to find *some* pressure distribution for which the boundary layer will overshoot (for instance, Goldberg's<sup>5</sup> case 3, for which incidentally the calculation method gives very good results) but it is surprising to find it happening in an 'equilibrium' power-law distribution. Since we are not dealing with a linear system we must not read too much into this curious phenomenon: in particular, it has nothing to do with the 'downstream instability' postulated by Clauser<sup>14</sup> for which no firm evidence has ever been found<sup>2</sup>. Physically, the increase in shear stress in the central part of the layer resulting from the sudden application of the pressure gradient causes an increase in shear-stress gradient over the inner layer, accentuated by the fall in  $c_f$ , which finally outweighs the pressure gradient and accelerates the flow near the wall causing  $c_f$  to rise and  $H$  to fall. The maximum shear stress attained during this process considerably exceeds the equilibrium value.

The variation of some of the integral parameters in this set of boundary layers is shown in Figs. 14 and 15. The results suggest that Nash's empirical assumption<sup>15</sup> of a unique relation between the profile parameter  $G$  and the dimensionless pressure gradient  $(\delta_1/\tau_w) dp/dx$  is not too far out for boundary layers in strong pressure gradients. Nash's assumption, that this unique relation is that indicated by measurements in equilibrium boundary layers, is *not* supposed to imply that the whole shear stress profile is determined by the local dimensionless pressure gradient. A quantitative conclusion from this series of calculations is that separation occurs when the initial value of the dimensionless pressure gradient  $(\delta_1/\tau_w) dp/dx$  exceeds 3, but that in milder pressure gradients equilibrium will eventually be attained. This figure will vary both with Reynolds number and with the exponent of the power-law pressure gradient. (For exponents more negative than about  $-0.3$ , equilibrium is not possible).

The behaviour of  $\delta_2$ , shown in Fig. 14c, merits some comment since the ratio of  $\delta_2$  at given  $x$  to the value at  $x = 24$  is larger for the thinner boundary layer – that is, those in milder dimensionless pressure gradients. (This effect would be even more marked if the calculations for different  $\delta_0$  had been done at the same  $U_{\text{ref}}/\nu$  instead of the same  $U_{\text{ref}} \delta_0/\nu$ , because  $c_f$  decreases with increasing  $\text{Re}$ ; also, the same effect can be seen in the experimental results of Fig. 5).

In zero pressure gradient,  $d\delta_2/dx$  would be not more than 0.00147 ( $c_f/2$  at  $x = 24$  in.) and this trend is shown on Fig. 14c using the value of  $\delta_0$  for the thinnest boundary layer. In strong adverse pressure gradient, with negligible surface shear stress, the momentum-integral equation integrates to give  $\delta_2 \propto U_1^{-(H+2)}$ , or  $\delta_2 \propto x$  taking  $H \approx 2$  and  $U_1 \propto x^{-0.25}$ : this line is also shown on Fig. 14c and agrees quite well with the calculations for the thickest three boundary layers. Evidently, the contribution of  $c_f$  to  $d\delta_2/dx$  in mild adverse pressure gradient results in a growth rate *larger* than in strong adverse pressure gradient where  $c_f$  is negligible; the effect would not be so noticeable at higher Reynolds numbers. The highest values of  $d\delta_2/dx$  occur in the equilibrium boundary layer far downstream: the approximate value shown in Fig. 14c is from Ref. 2.

The velocity profiles for the last five output stations of each calculation are plotted in the form  $U/u_\tau$  against  $u_\tau y/\nu$  in Fig. 16. The logarithmic region seems to vanish (i.e. its outer boundary decreases to

$u_\tau y/\nu = 30$ ) at about  $(\nu/u_\tau^3)\partial\tau/\partial y = 0.01$ , the value often quoted: this implies  $(y/\tau_w)d\tau/dy = 0.3$  at  $u_\tau y/\nu = 30$ , so that the departure from the logarithmic law predicted by Townsend's mixing-length formula is  $0.35 u_\tau$  (about the smallest departure that would be noticeable in practice). Evidently, Townsend's formula, which neglects advection, is sufficiently accurate in practice to predict the departure from the logarithmic law provided that the true shear-stress gradient is used: it cannot be equated to the pressure gradient. Once the logarithmic region disappears, Townsend's formula becomes invalid since the logarithmic law provides a constant of integration.

#### *Conclusions.*

1. Measurements of velocity profiles and surface shear stress in three aerofoil-type boundary layers should be useful as test cases for calculation methods.
2. Further turbulence measurements in one of these layers show that advection of turbulent energy is fairly small except near the outer edge of the boundary layer where it is supplied by diffusion. Thus production and dissipation are nearly equal and the mixing length is nearly equal to the dissipation length parameter which is known to be a nearly universal function. This explains why calculation methods assuming a universal mixing-length distribution are reasonably successful in aerofoil boundary layers.
3. The investigation has been extended to a wider range of pressure gradients by doing calculations by a method which is believed to be generally reliable. The results show that a boundary layer passing from one equilibrium state to another does not necessarily do so monotonically.
4. It is suggested that further general studies of boundary-layer development will be less useful than experiments designed to investigate particular turbulence phenomena.

#### *Acknowledgements.*

Most of the experimental work reported here was done by Mr. M. G. Terrell. Mr. D. H. Ferriss programmed the computer calculations.

## LIST OF SYMBOLS

$c_f$	$\tau_w/\frac{1}{2}\rho U_1^2$ , surface shear-stress coefficient
$c_p$	$(U_1/U_{ref})$
$G$	$(2/c_f)^{\frac{1}{2}}(1-H^{-1})$ , defect profile parameter
$H$	$\delta_1/\delta_2$
$L$	$(\tau/\rho)^{3/2}/\epsilon$ , dissipation-length parameter
$l$	$(\tau/\rho)^{\frac{1}{2}}/(\partial U/\partial y)$ , mixing length
$p$	Static pressure
$\overline{q^2}$	$\overline{u^2} + \overline{v^2} + \overline{w^2}$
$U, V$	Mean velocity components
$U_{ref}$	Tunnel reference speed, 120 ft/sec
$u, v, w$	Fluctuating velocity components
$x$	Distance from leading edge
$y$	Distance normal to surface
$\delta_1$	Displacement thickness
$\delta_2$	Momentum thickness
$\delta_{99.5}$	Distance from surface at which $U/U_1 = 0.995$
$\epsilon$	Rate of dissipation of turbulent energy into heat
$\nu$	Kinematic viscosity
$\nu_\tau$	$(\tau/\rho)/(\partial U/\partial y)$ , eddy kinematic viscosity
$\rho$	Density
$\tau$	Reynolds shear stress $-\rho \overline{uv}$
<i>Suffixes</i>	
$w$	wall
$1$	Free stream

## REFERENCES

- | <i>No.</i> | <i>Author(s)</i>                            | <i>Title, etc.</i>  |
|------------|---|---|
| 1          | P. Bradshaw and D. H. Ferriss               | The response of a retarded equilibrium turbulent boundary layer to the sudden removal of pressure gradient.<br>NPL Aero Report 1145. A.R.C. 26 758. March 1965. |
| 2          | P. Bradshaw                                 | The turbulence structure of equilibrium boundary layers.<br><i>J. Fluid Mech.</i> 29, 625 (1967).   |
| 3          | P. Bradshaw, D. H. Ferriss and N. P. Atwell | Calculation of boundary-layer development using the turbulent energy equation.<br><i>J. Fluid Mech.</i> 28, 593 (1967).   |
| 4          | J. F. Nash and P. Bradshaw                  | The magnification of roughness drag by pressure gradients.<br><i>J. R. aero. Soc.</i> 71, 44 (1967).  |
| 5          | P. Goldberg                                 | Upstream history and apparent stress in turbulent boundary layers.<br>M.I.T. Gas Turbine Lab. Rep. 85 (1966).   |
| 6          | H. L. Moses                                 | The behaviour of turbulent boundary layers in adverse pressure gradients.<br>M.I.T. Gas Turbine Lab. Rep. 73 (1964).  |
| 7          | P. Bradshaw and G. E. Hellens               | The NPL in. x 9 in. boundary-layer tunnel.<br>A.R.C. R. & M. 3437. October 1964.  |
| 8          | P. Bradshaw and R. F. Johnson               | Turbulence measurements with hot wire anemometers.<br>NPL Note on Applied Science 33 (1963).  |
| 9          | M. R. Head and I. Rechenberg                | The Preston tube as a means of measuring skin friction.<br><i>J. Fluid Mech.</i> 14, 1 (1962).  |
| 10         | P. Bradshaw and P. V. Galea                 | Step-induced separation of a turbulent boundary layer in incompressible flow.<br><i>J. Fluid Mech.</i> 27, 111 (1967).  |
| 11         | A. A. Townsend                              | Equilibrium layers and wall turbulence.<br><i>J. Fluid Mech.</i> 11, 97 (1961).   |
| 12         | P. Bradshaw                                 | "Inactive" motion and pressure fluctuations in turbulent boundary layers<br><i>J. Fluid Mech.</i> 30, 241 (1967).   |
| 13         | F. H. Clauser                               | Turbulent boundary layers in adverse pressure gradients.<br><i>J. aero. Sci.</i> 21, 91 (1954).   |
| 14         | G. L. Mellor                                | The effect of pressure gradients on turbulent flow near a smooth wall.<br><i>J. Fluid Mech.</i> 24, 255 (1966).   |
| 15         | J. F. Nash and A. G. J. Macdonald           | The calculation of momentum thickness in a turbulent boundary layer at Mach numbers up to unity.<br>A.R.C. C.P. 963. July 1966.                                 |
| 16         | B. G. J. Thompson                           | A new two-parameter family of mean velocity profiles for incompressible turbulent boundary layers on smooth walls.<br>A.R.C. R. & M. 3463. April 1965.          |

REFERENCES—*continued*

- | <i>No.</i> | <i>Author(s)</i>                               | <i>Title, etc.</i>   |
|------------|--|--|
| 17         | H. Ludwig and W. Tillman . .                   | Investigation of the wall shearing stress in turbulent boundary layers.<br>NACA TM 1285 (1949).        |
| 18         | J. F. Nash and . . . . .<br>A. G. J. Macdonald | A turbulent skin-friction law for use at subsonic and transonic speeds.<br>A.R.C. C.P. 948. July 1966. |
-

	$x$	24	30	36	42	48	60	72	84	
Layer A	$c_p$	1.096	1.008	0.916	0.852	0.797	0.714	0.651	0.600	
	$\delta_1$	0.0806	0.1054	0.1512	0.1907	0.2107	0.2733	0.3549	0.4354	
	$\delta_2$	0.0552	0.0747	0.1042	0.1271	0.1405	0.1865	0.2409	0.2912	
	$H$	1.460?	1.411	1.451	1.500	1.500	1.465	1.472	1.495	
	$\delta_{995}$	0.470	0.565	0.775	0.870	1.034	1.340	1.715	2.075	
	$cf$	0.00295	0.00260	0.00227	0.00214	0.00207	0.00195	0.00188	0.00184	
	$\frac{\delta_1}{\tau_w} \frac{dp}{dx}$	0.364	0.540	0.950	1.080	1.080	1.190	1.340	1.440	
	$G$	8.22	8.10	9.22	10.20	10.40	10.20	10.50	10.90	
	$c_f(T)$		0.00275	0.00230	0.00205	0.00200	0.00198	0.00187	0.00175	(Thompson <sup>16</sup> )
	$c_f(L-T)$		0.00281	0.00241	0.00217	0.00214	0.00212	0.00199	0.00179	(Ludwig-Tillman <sup>17</sup> )
$c_f(N-M)$		0.00268	0.00233	0.00207	0.00203	0.00205	0.00192	0.00178	(Nash-Macdonald <sup>18</sup> )	
$\frac{U_1 \delta_2}{\nu}$	3670	4733	6328	7386	7895	9919	12134	14257		
Layer B	$\delta_1'$	0.1244	0.157	0.200	0.250	0.286	0.375	0.469	0.556	
	$\delta_2$	0.0884	0.112	0.137	0.168	0.195	0.255	0.315	0.367	
	$H$	1.407	1.400	1.462	1.488	1.467	1.471	1.488	1.515	
	$\delta_{995}$	0.693	0.877	1.066	1.240	1.394	1.740	2.100	2.500	
	$c_f$	0.002575	0.00235	0.00207	0.00195	0.00188	0.00173	0.00165	0.00166	
	$\frac{\delta_1}{\tau_w} \frac{dp}{dx}$	0.640	1.140	1.370	1.556	1.617	1.842	2.012	2.034	
	$G$	8.05	8.33	9.82	10.50	10.38	10.89	11.42	11.80	
	$c_f(T)$	0.00255	0.00240	0.00210	0.00205	0.00192	0.00181	0.00170	0.00159	

	24	30	36	42	48	60	72	84	
Layer C	$c_f(L-T)$	0.00272	0.00260	0.00223	0.00205	0.00205	0.00193	0.00179	0.00167
	$c_f(N-M)$	0.00254	0.00243	0.00214	0.00196	0.00195	0.00184	0.00176	0.00164
	$\frac{U_1 \delta_2}{\nu}$	5923	7447	8391	9924	11157	13791	16269	18203
Layer C	$\delta_1$	0.177	0.216	0.272	0.332	0.376	0.487	0.606	0.697
	$\delta_2$	0.130	0.154	0.199	0.227	0.259	0.329	0.395	0.451
	$H$	1.361	1.403	1.370	1.466	1.451	1.477	1.532	1.543
	$\delta_{995}$	1.125	1.350	1.550	1.740	1.900	2.300	2.700	3.100
	$c_f$	0.00251	0.00225	0.00200	0.00187	0.00180	0.00166	0.00153	0.00147
	$\frac{\delta_1 dp}{\tau_w dx}$	0.942	1.632	1.928	2.155	2.219	2.495	2.807	2.876
	$G$	7.50	8.56	8.54	10.39	10.36	11.21	12.58	12.98
	$c_f(T)$	0.00250	0.00220	0.00222	0.00186	0.00183	0.00169	0.00150	0.00145
	$c_f(L-T)$	0.00258	0.00234	0.00233	0.00195	0.00195	0.00178	0.00157	0.00151
	$c_f(N-M)$	0.00250	0.00225	0.00227	0.00188	0.00188	0.00174	0.00154	0.00148
	$\frac{U_1 \delta_2}{\nu}$	8711	9895	12188	13409	14819	17792	20400	22370

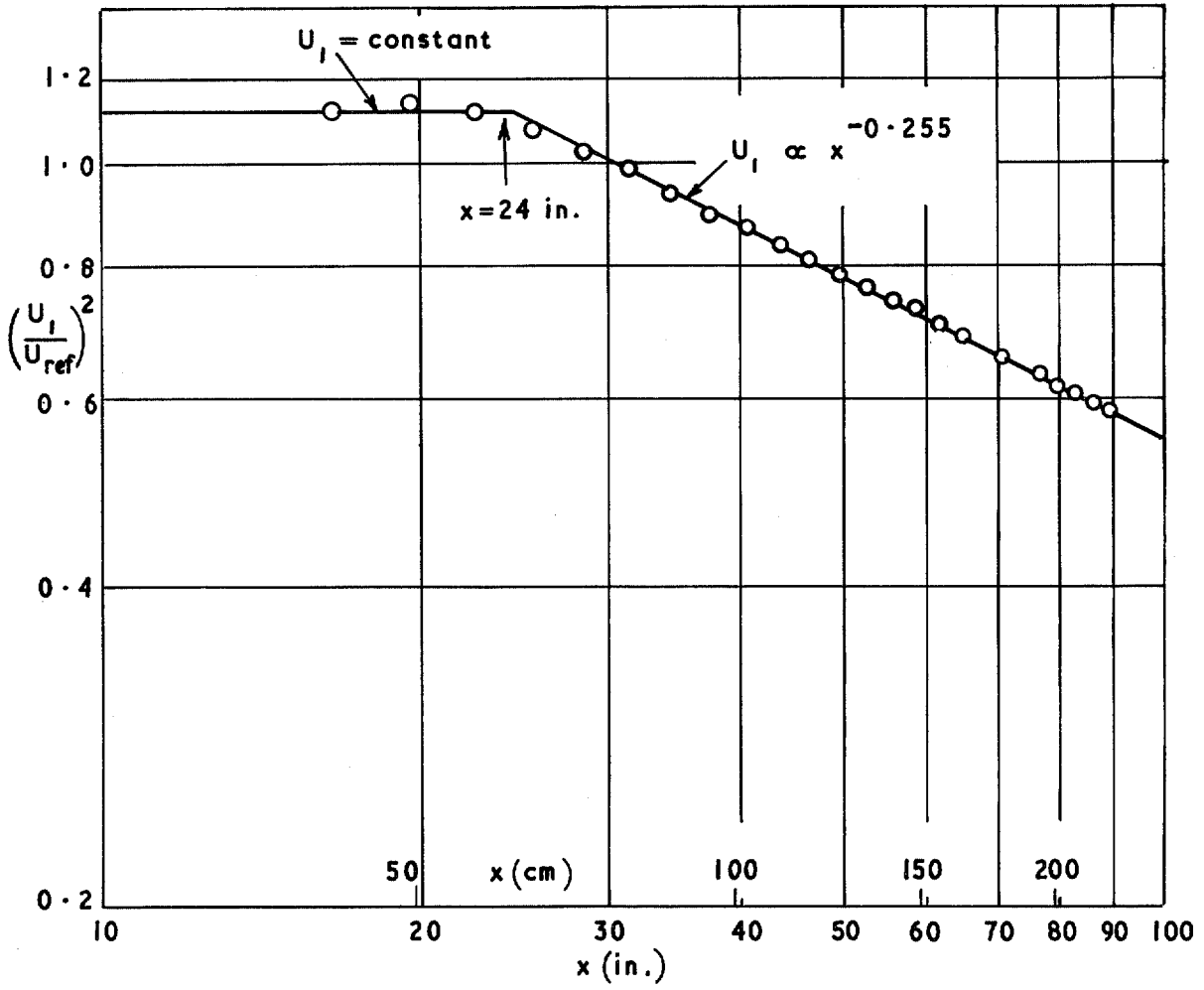


FIG. 1. Pressure distribution.

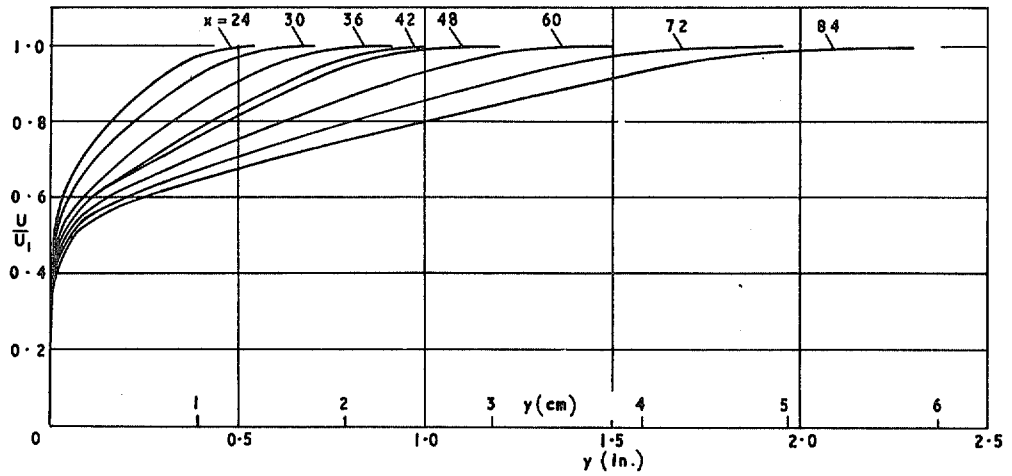


FIG. 2a. Mean velocity profiles; boundary layer 'A'.

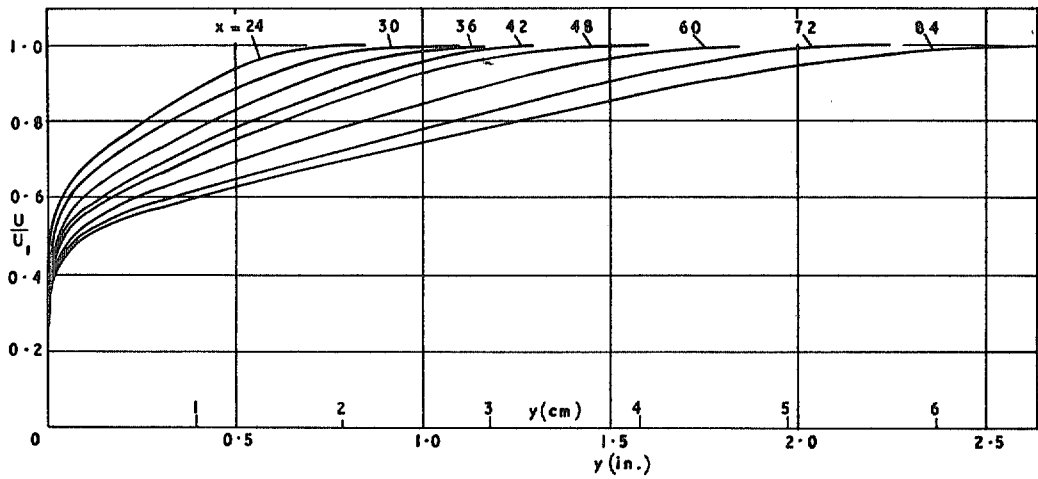


FIG. 2b. Mean velocity profiles; boundary layer 'B'.

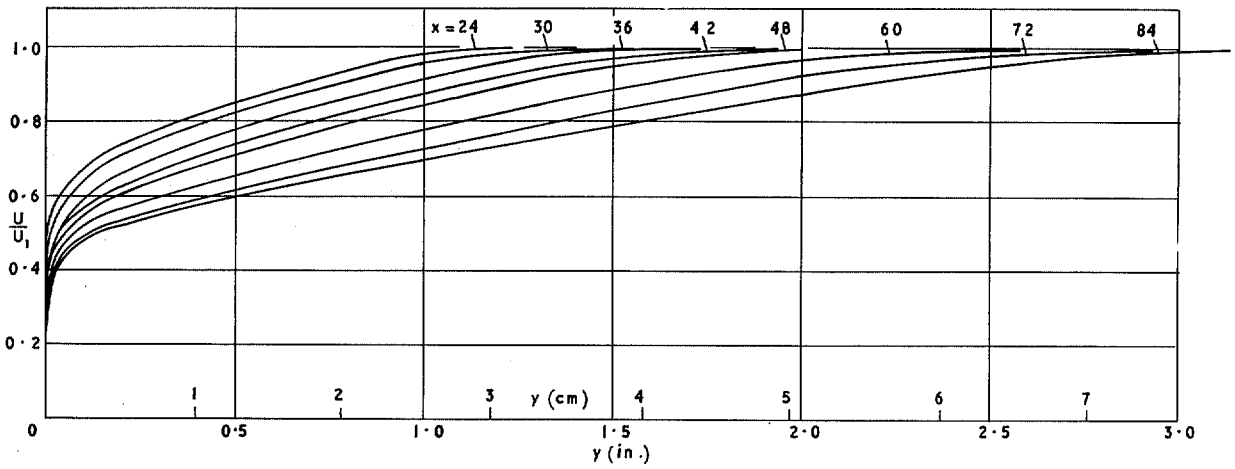


FIG. 2c. Mean velocity profiles; boundary layer 'C'.

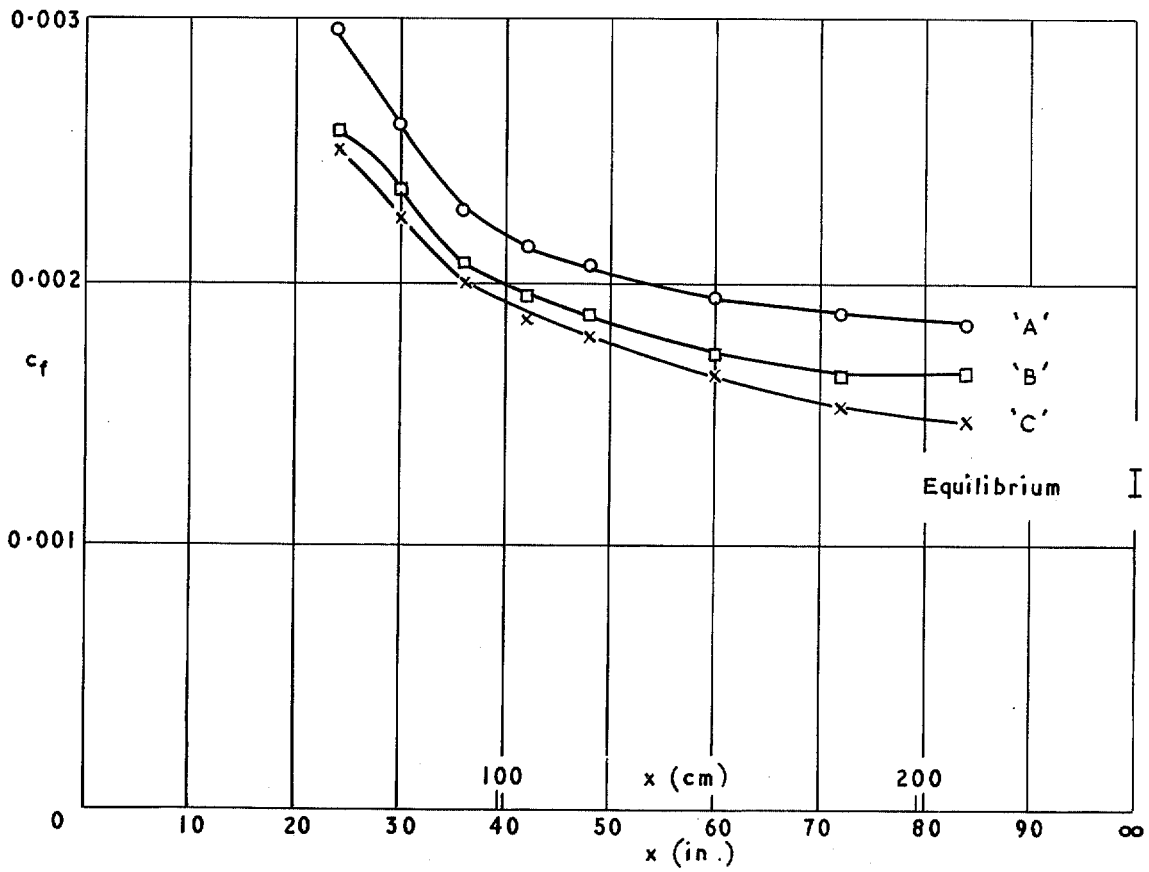


FIG. 3. Surface shear-stress coefficient.

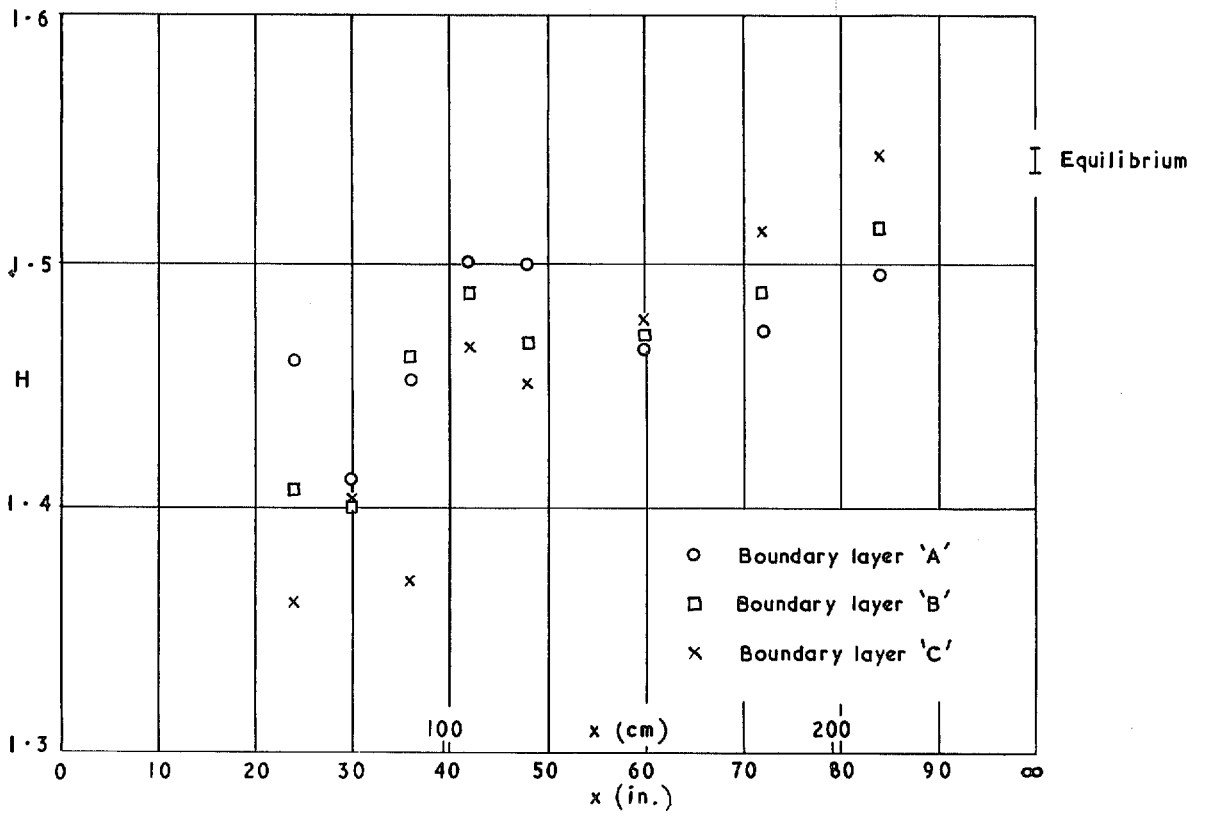


FIG. 4. Profile parameter  $H$ .

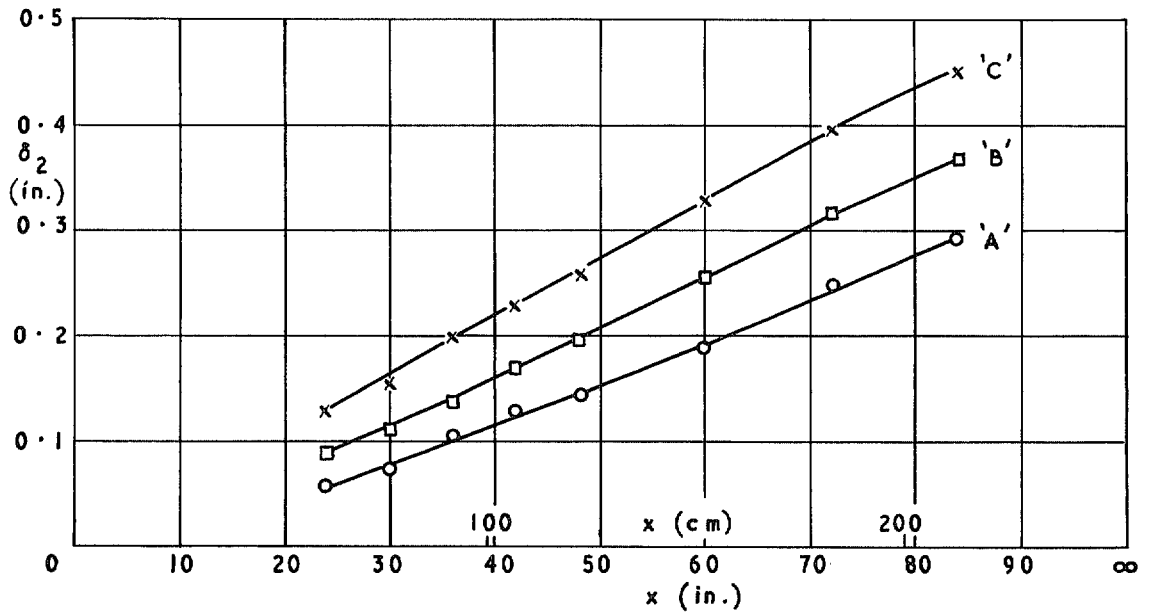


FIG. 5. Momentum thickness.

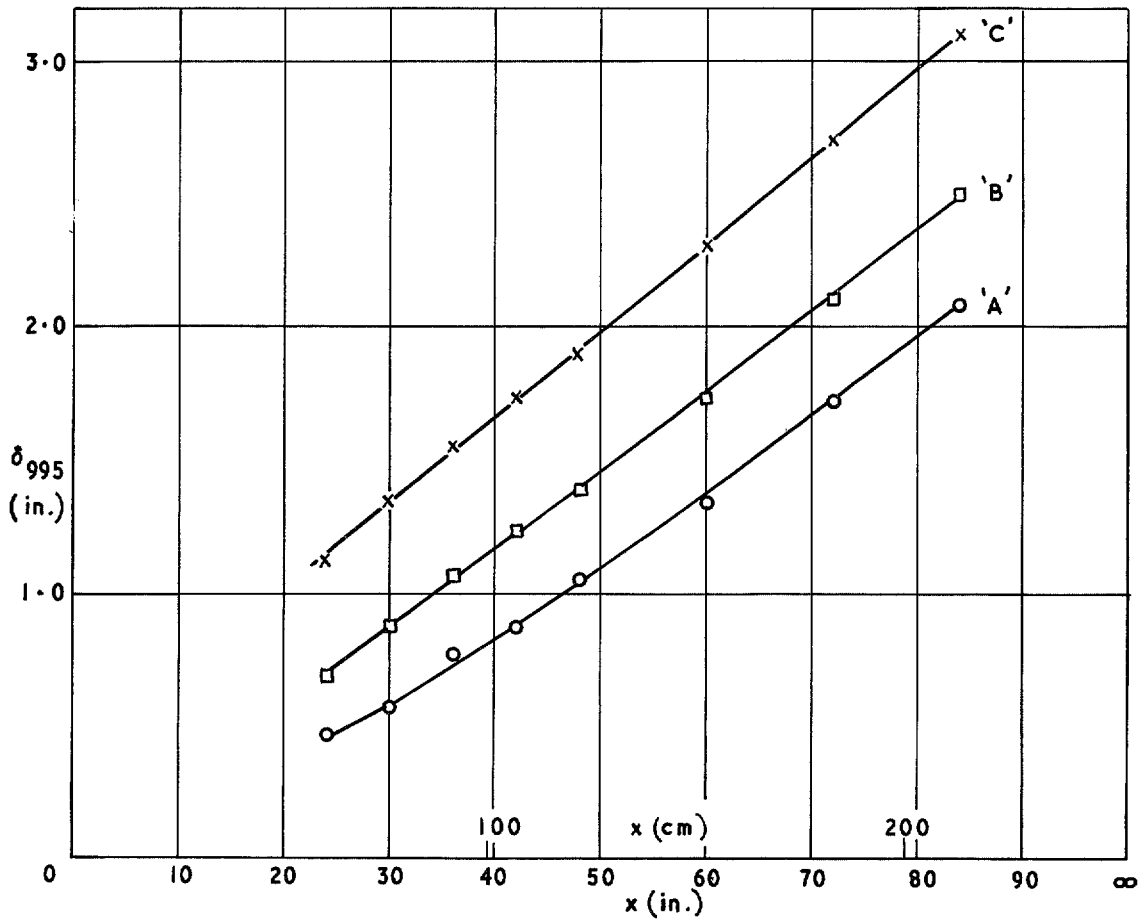


FIG. 6. Boundary-layer thickness.

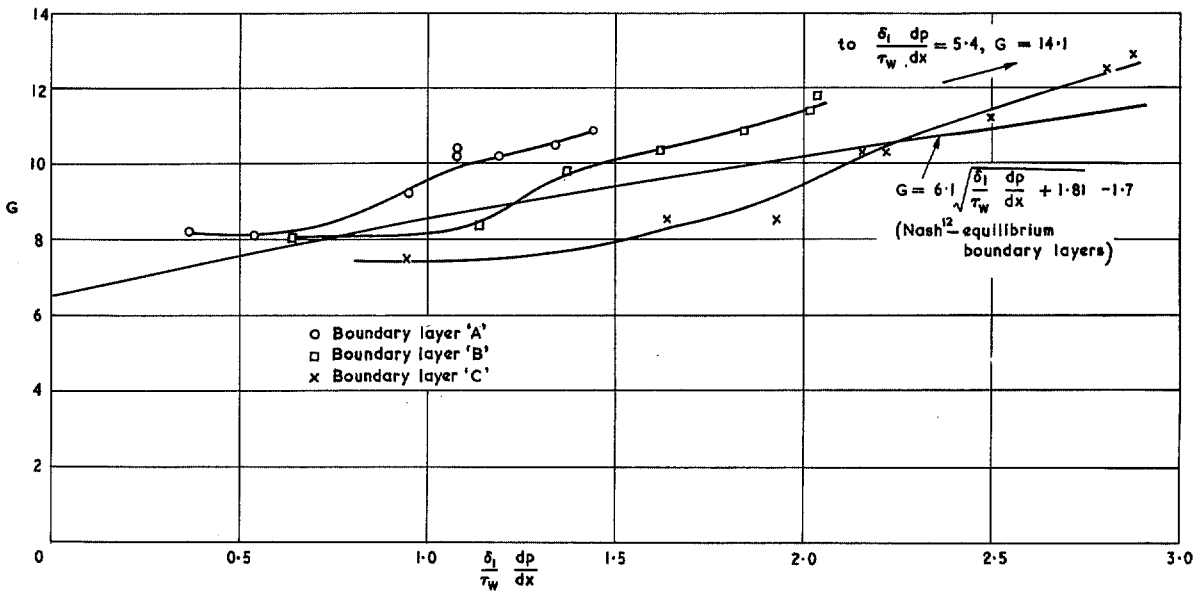


FIG. 7. Defect profile parameter vs. dimensionless pressure gradient.

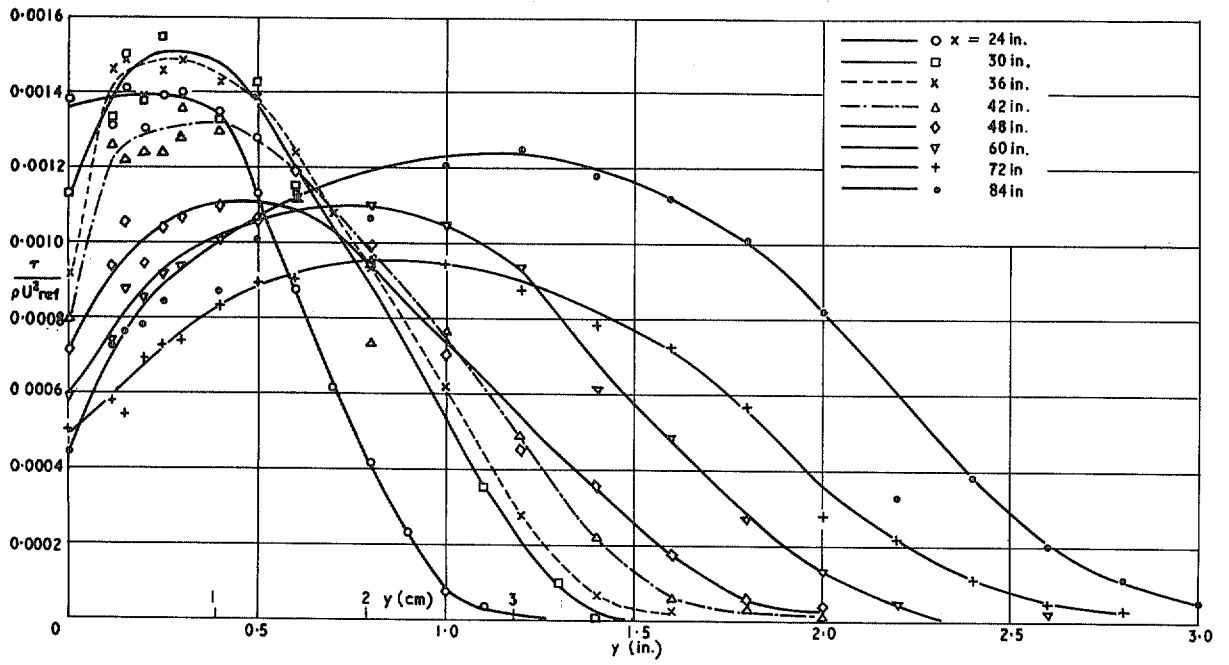


FIG. 8. Shear-stress profiles; boundary layer 'C'.

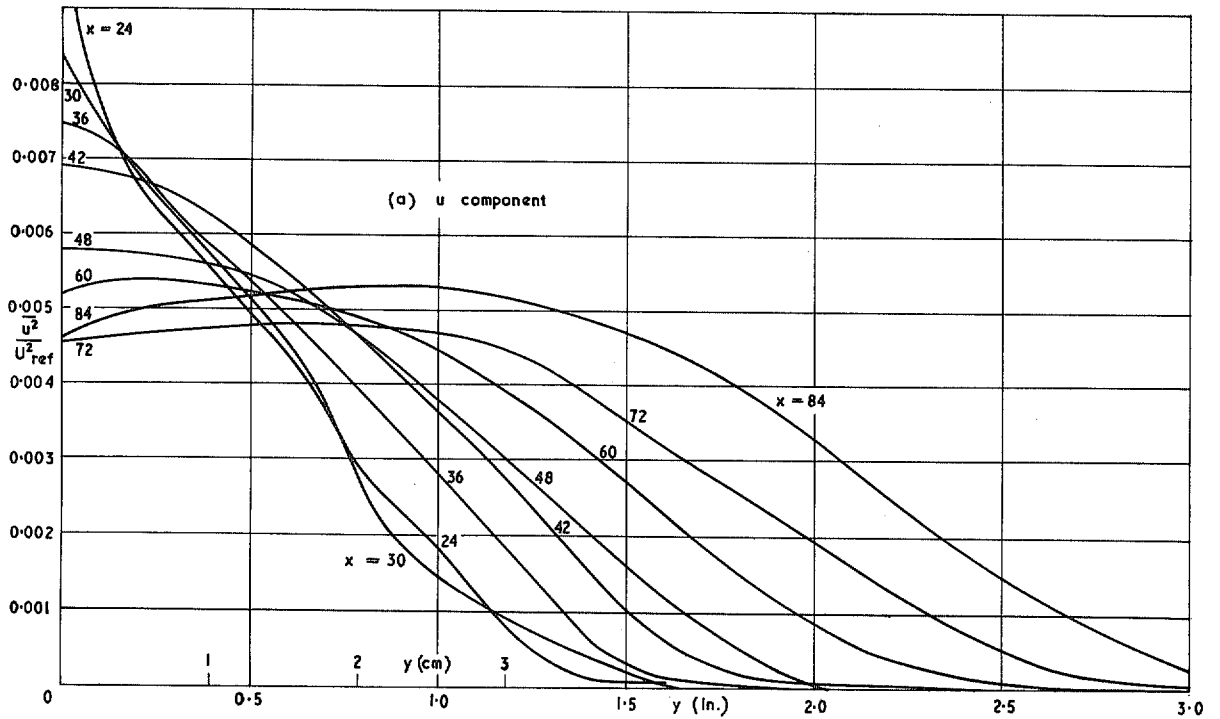


FIG. 9a. Turbulent intensity profiles; boundary layer 'C'.

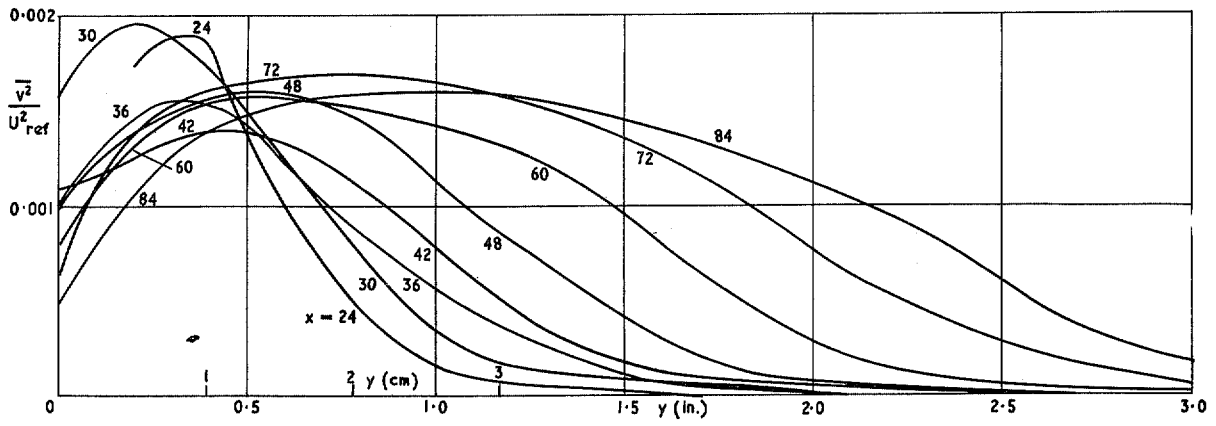


FIG. 9b. Turbulent intensity profiles, boundary layer 'C';  $v$ -component.

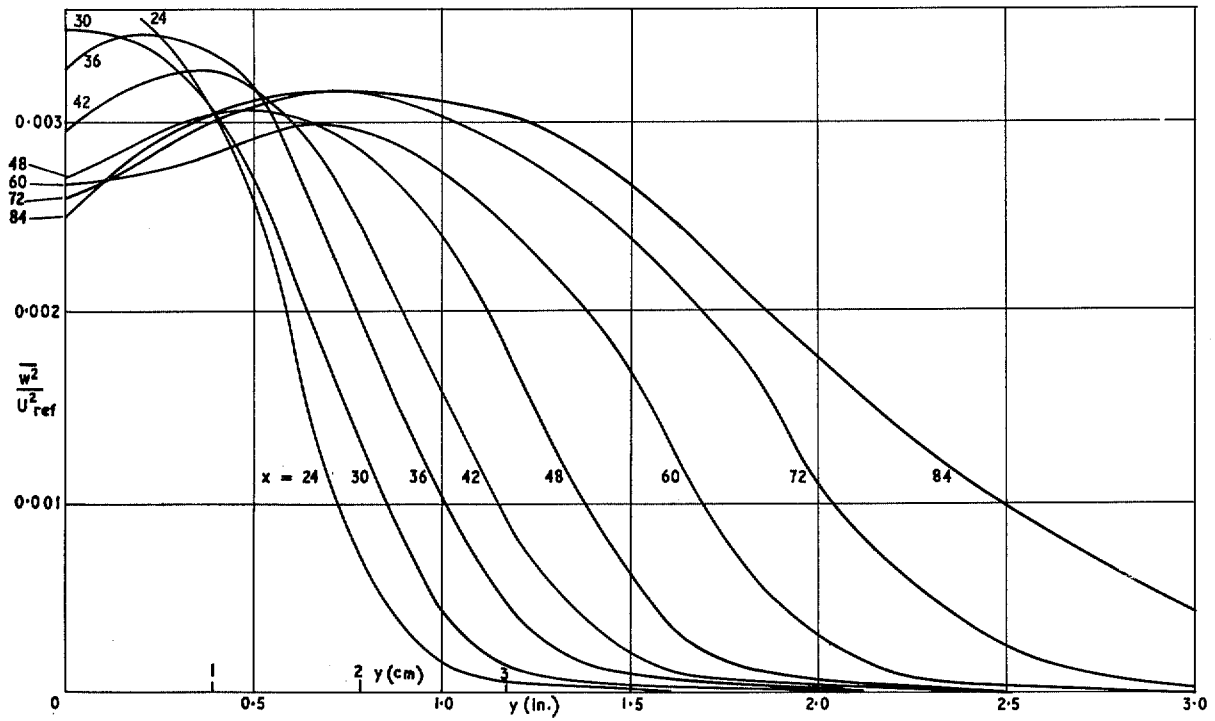


FIG. 9c. Turbulent intensity profiles, boundary layer 'C';  $w$ -component.

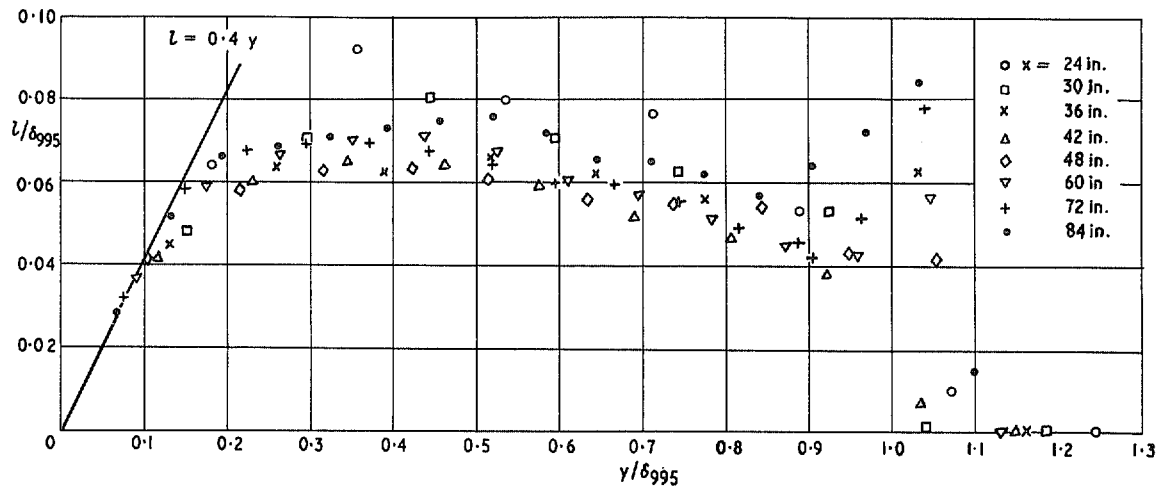


FIG. 10. Mixing length; boundary layer 'C'.

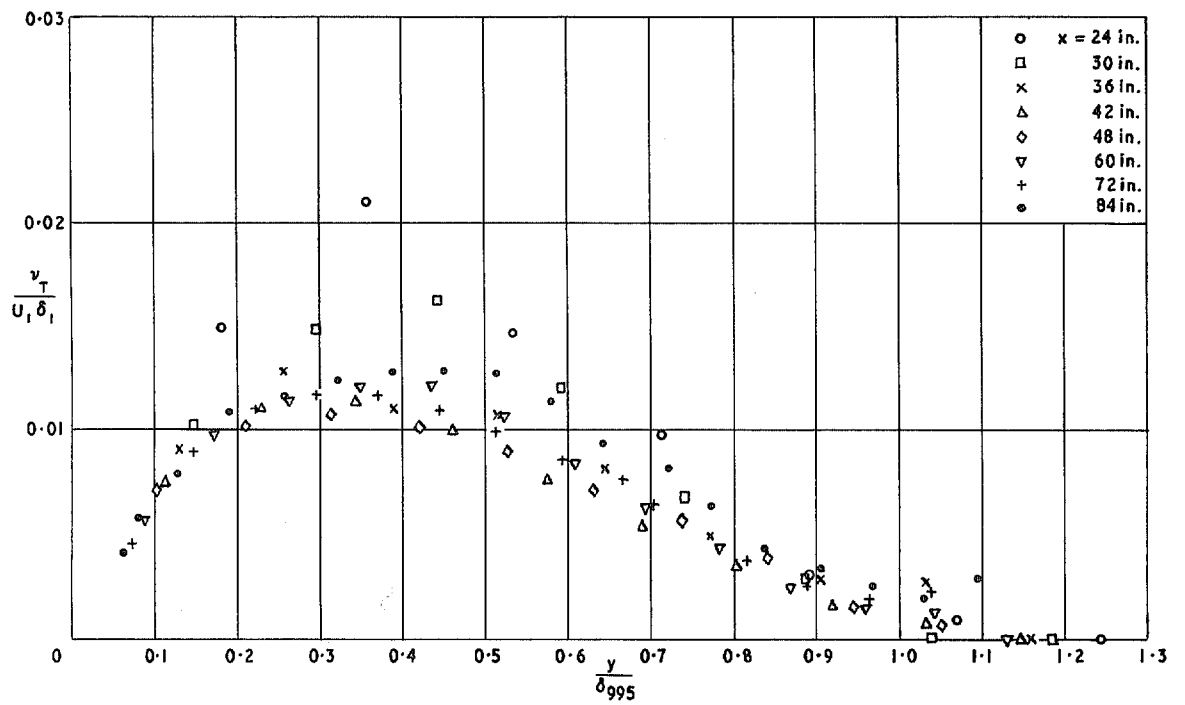


FIG. 11. Eddy viscosity ~ boundary layer 'C'.

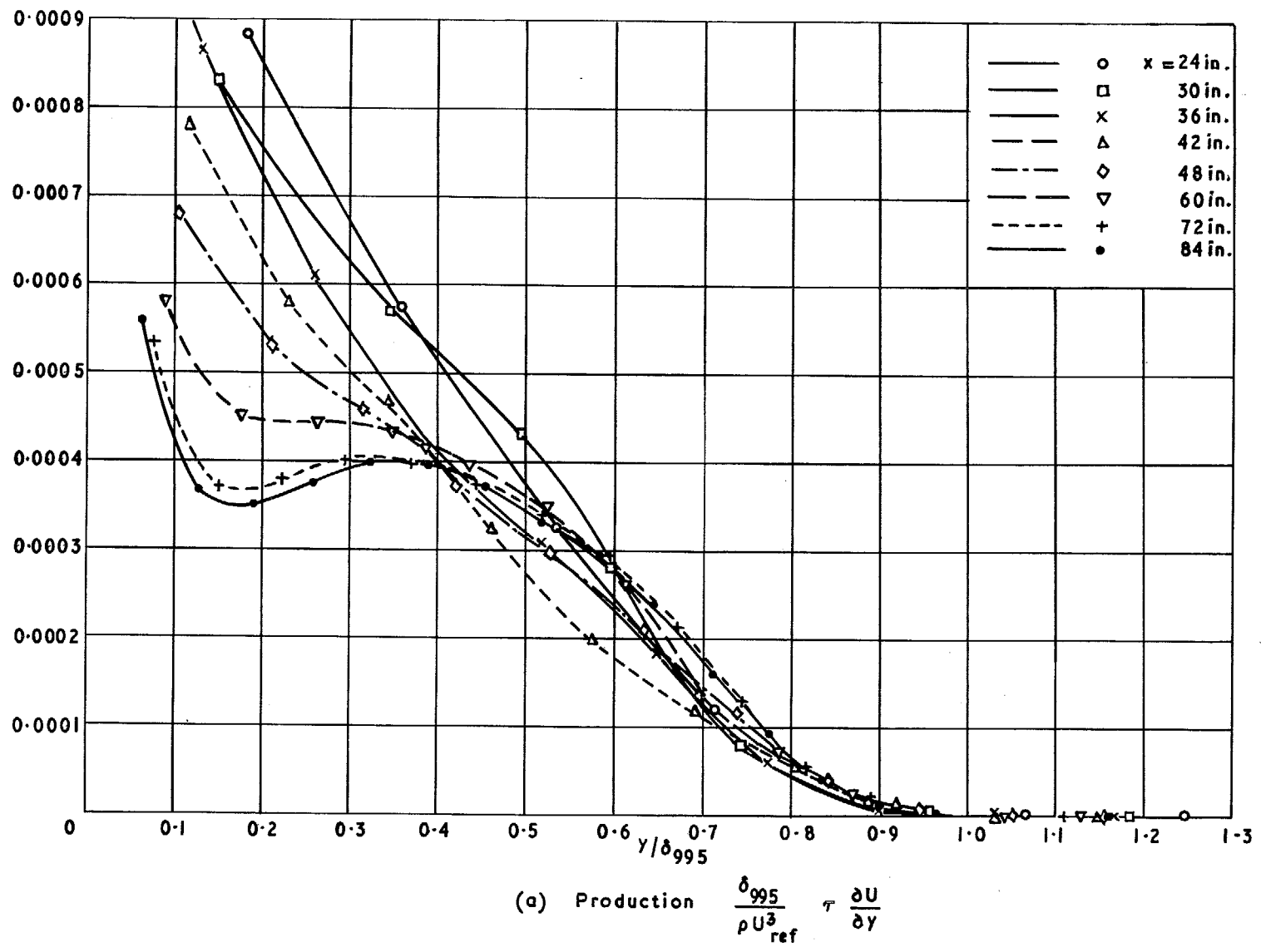


FIG. 12a. Turbulent kinetic energy balance in boundary layer 'C'.

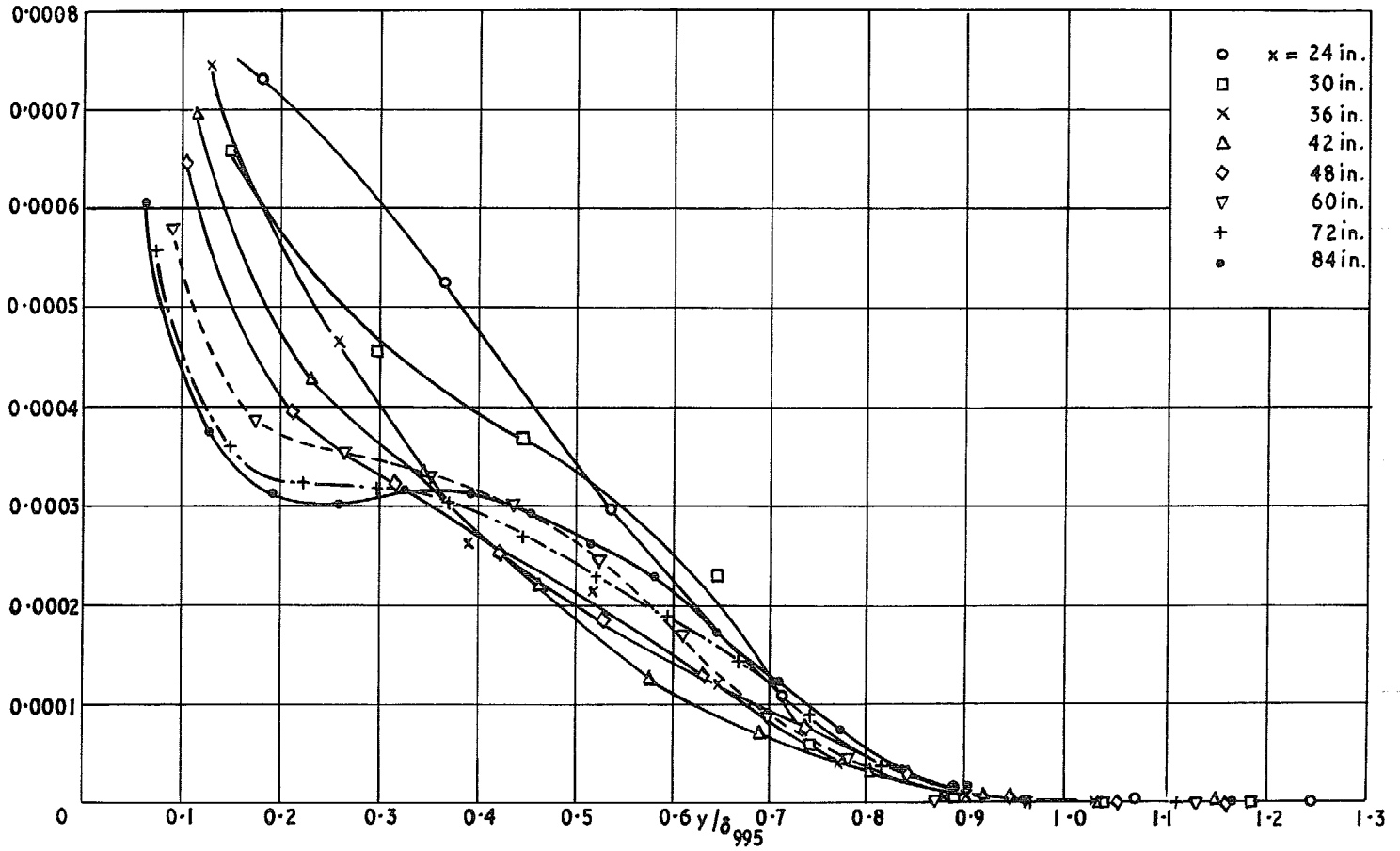


FIG. 12b. Approximate dissipation  $\frac{\delta_{995}}{U_{ref}^3} \frac{(\tau/\rho)^{3/2}}{L} \approx \frac{\delta_{995}}{U_{ref}^3} \varepsilon$ . (See Fig. 13).

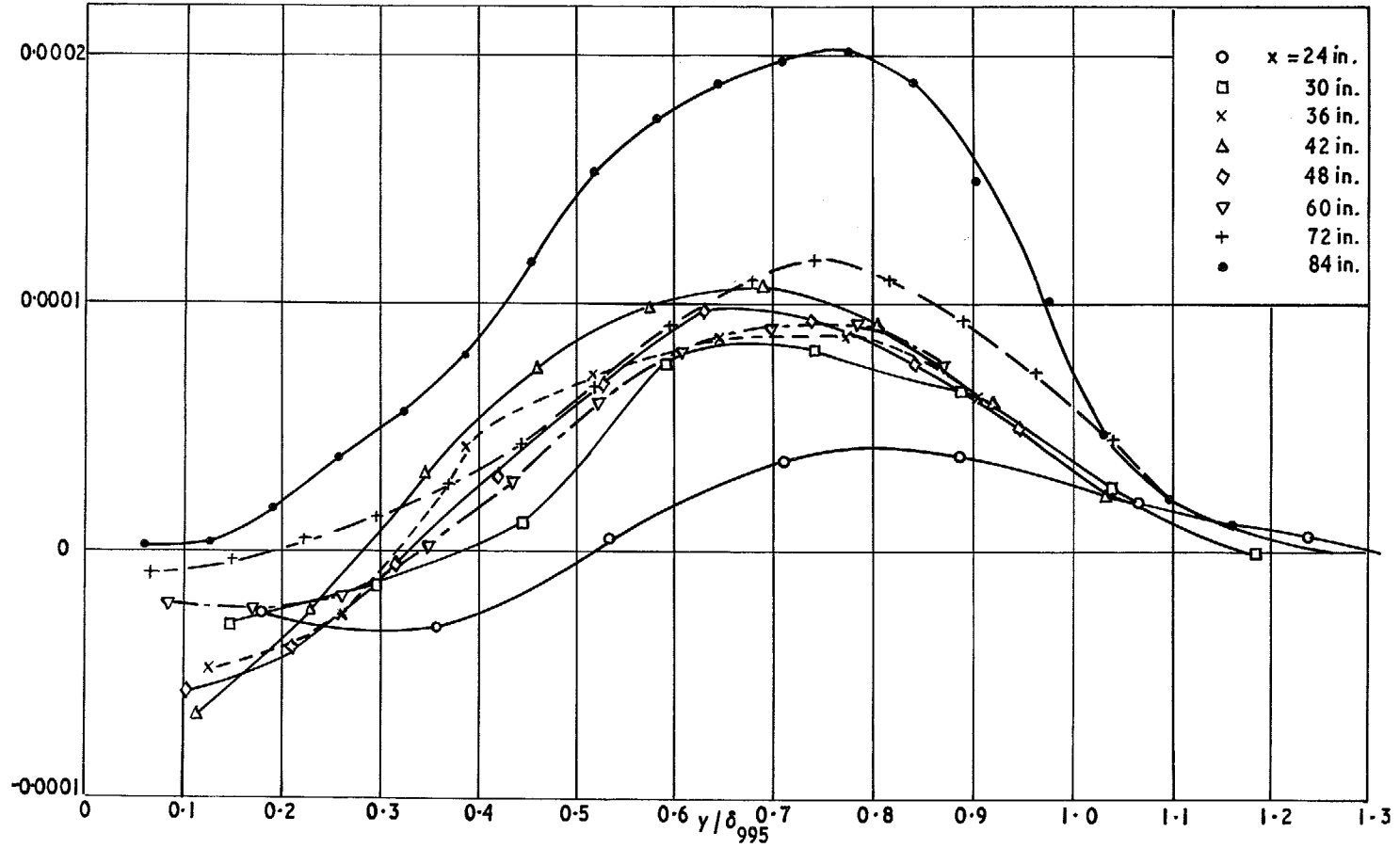


FIG. 12c. Advection  $\frac{\delta_{995}}{U_{\text{ref}}^3} \left( U \frac{\partial}{\partial x} + V \frac{\partial}{\partial y} \right) \frac{1}{2} \overline{q^2}$ .

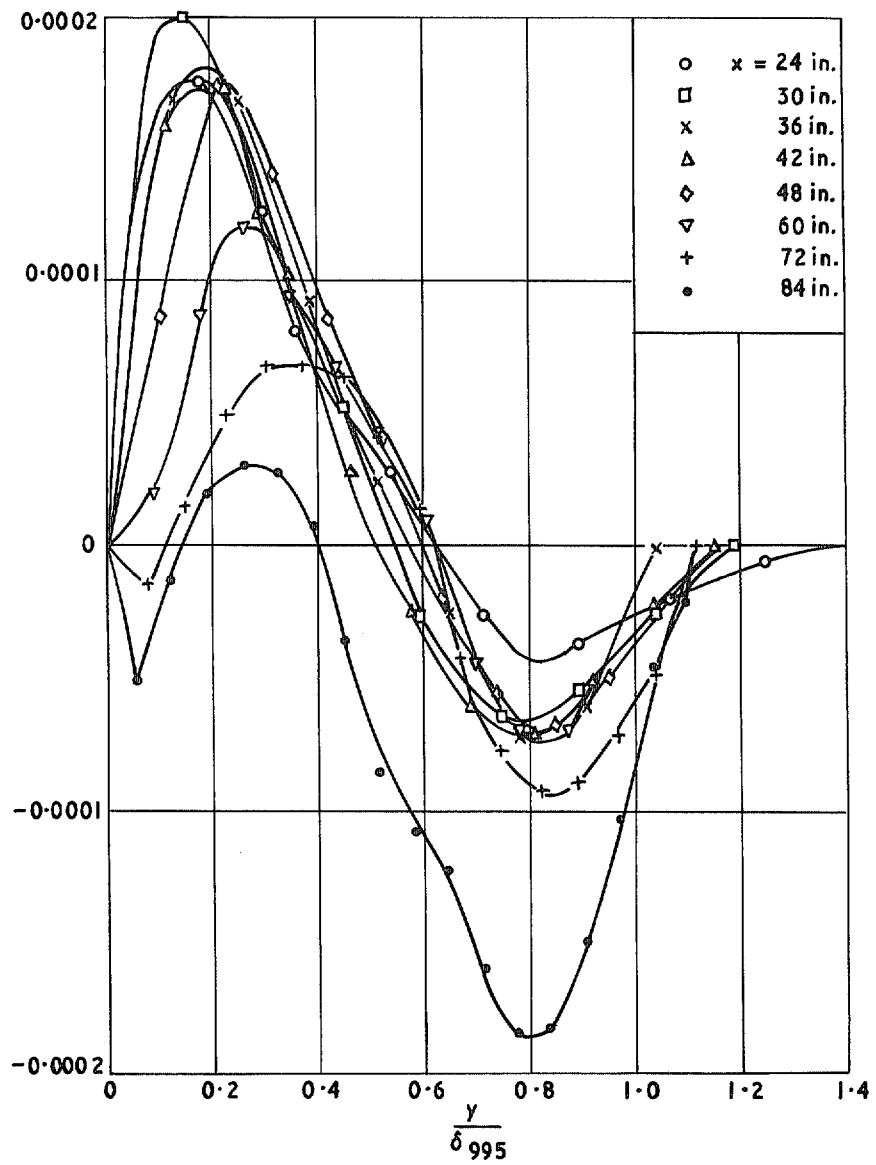


FIG. 12d. Diffusion  $\frac{\delta_{995}}{\rho U_{ref}^3} \frac{\partial}{\partial y} \left( p\bar{v} + \frac{1}{2}\rho \overline{q^2v} \right)$  by difference.

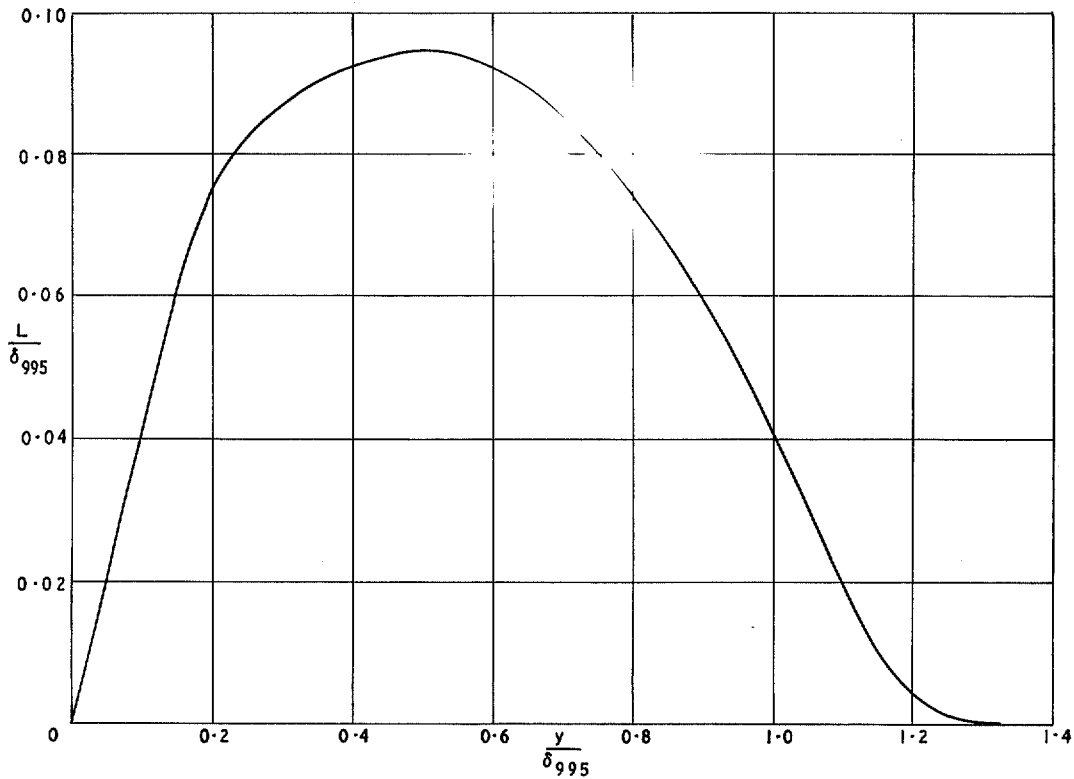


FIG. 13. Dissipation length parameter  $L \equiv \left( \frac{\tau/\rho}{\tau} \right)$ .

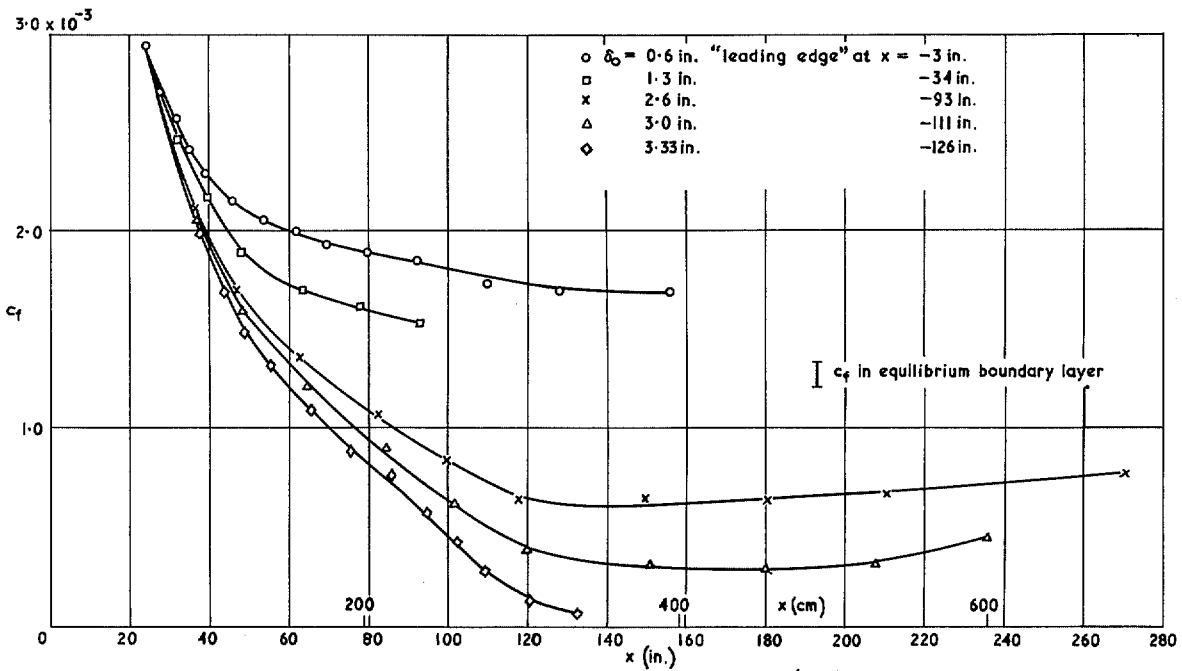


FIG. 14a. Calculations for different initial boundary-layer thicknesses,  $\frac{U_1 \delta_0}{\nu} = 40\,000$  in all cases: shear-stress coefficient.

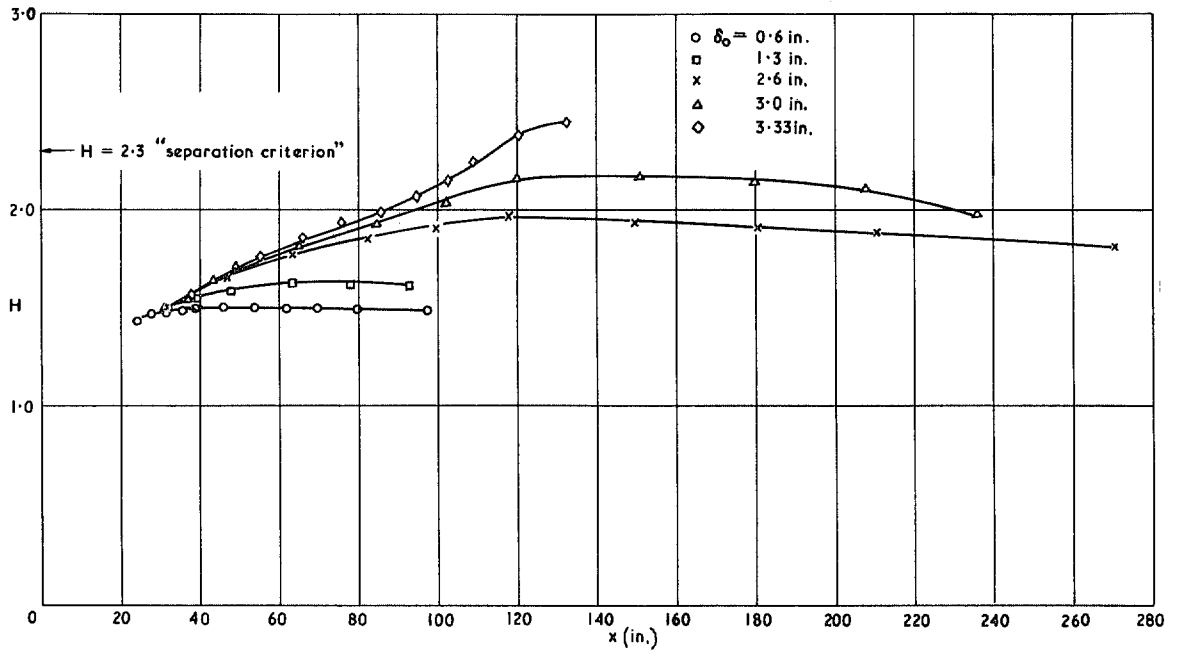


FIG. 14b. Shape parameter  $H$ .

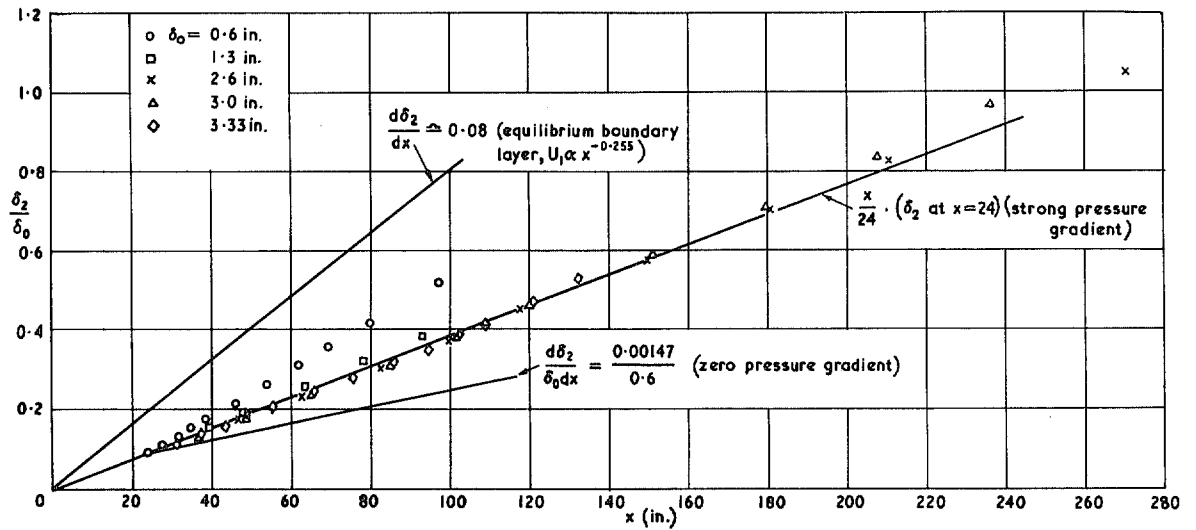


FIG. 14c. Momentum thickness.

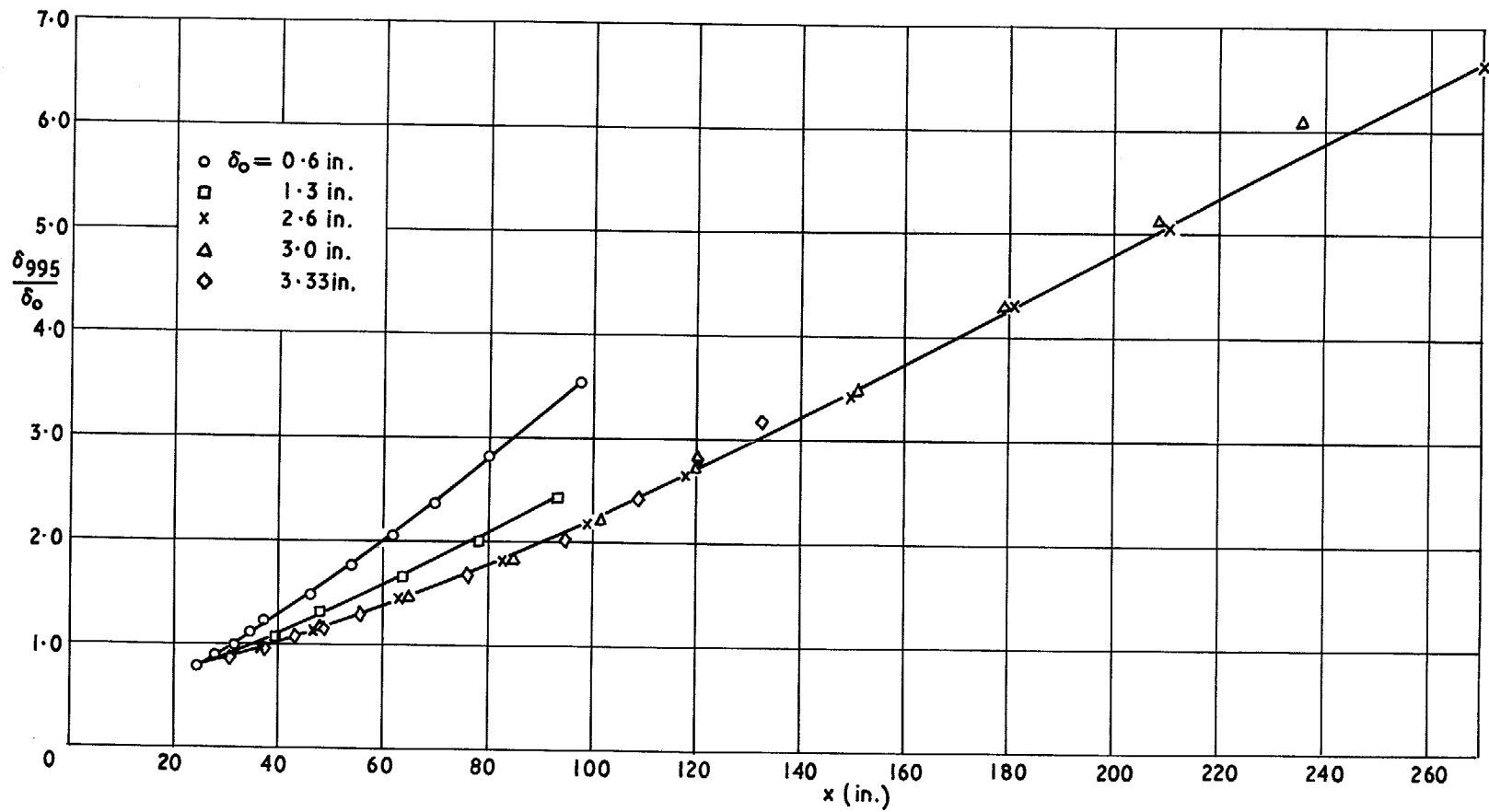


FIG. 14d. Boundary layer thickness.

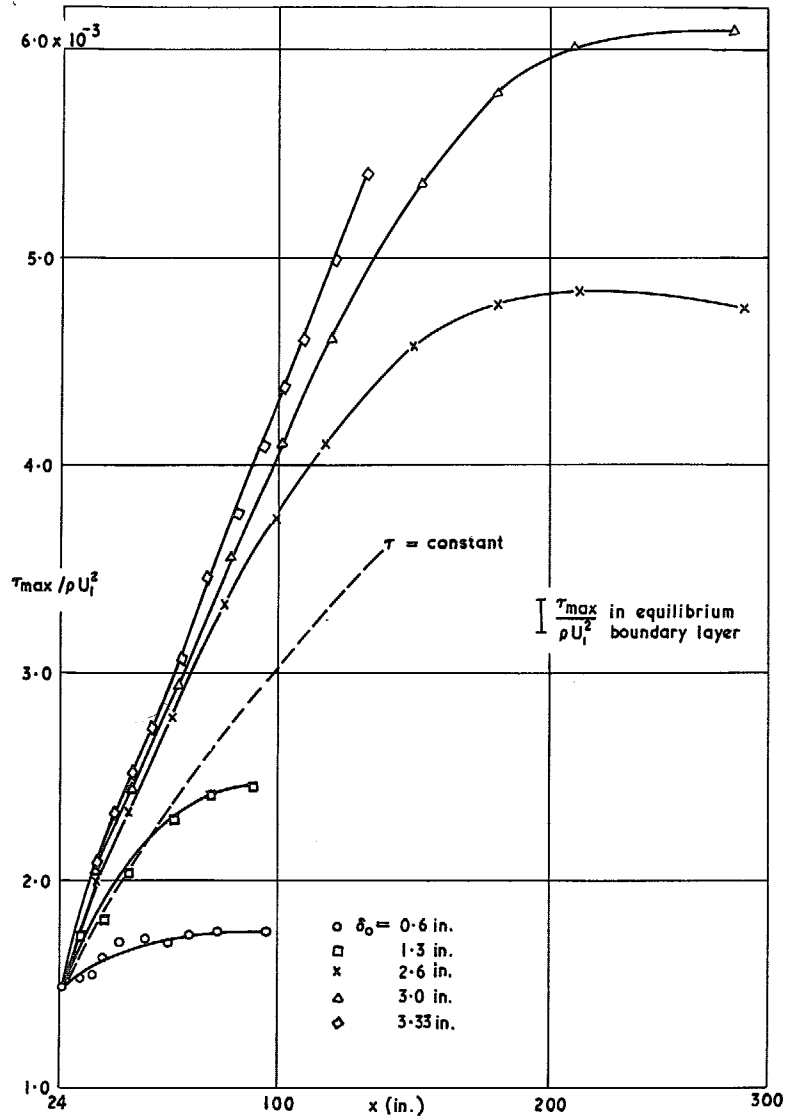


FIG. 14e. Maximum shear stress.

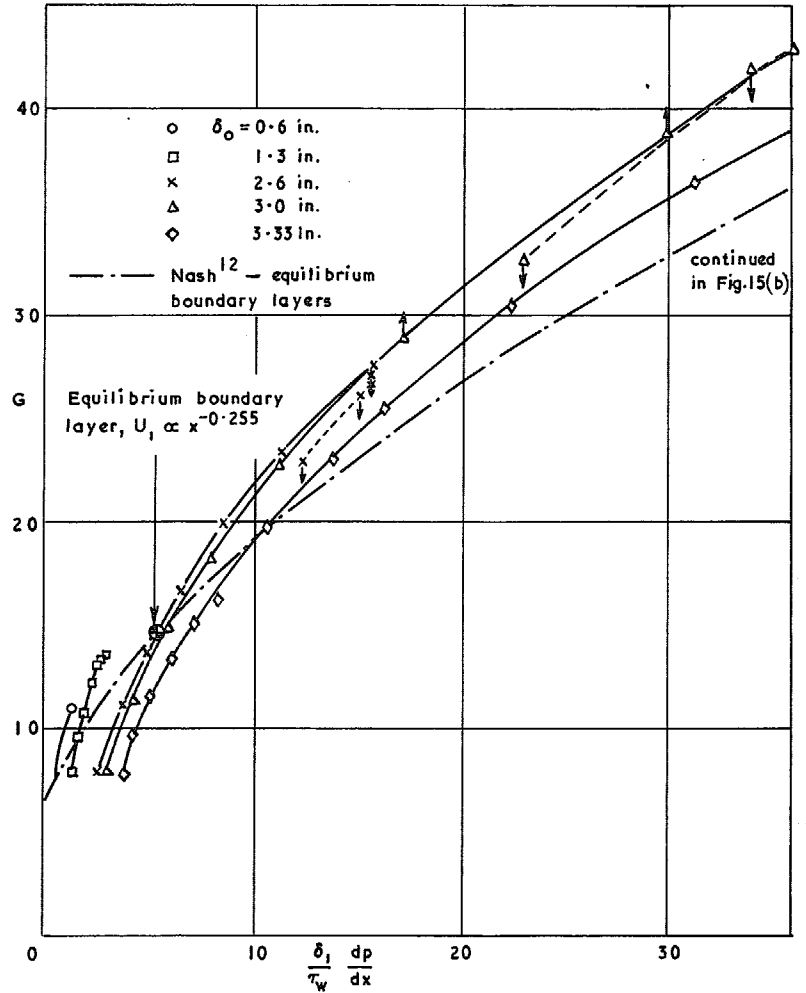


FIG. 15a. Defect profile parameter vs. dimensionless pressure gradient.

$$\text{Small } \frac{\delta_1}{\tau_w} \frac{dp}{dx}$$

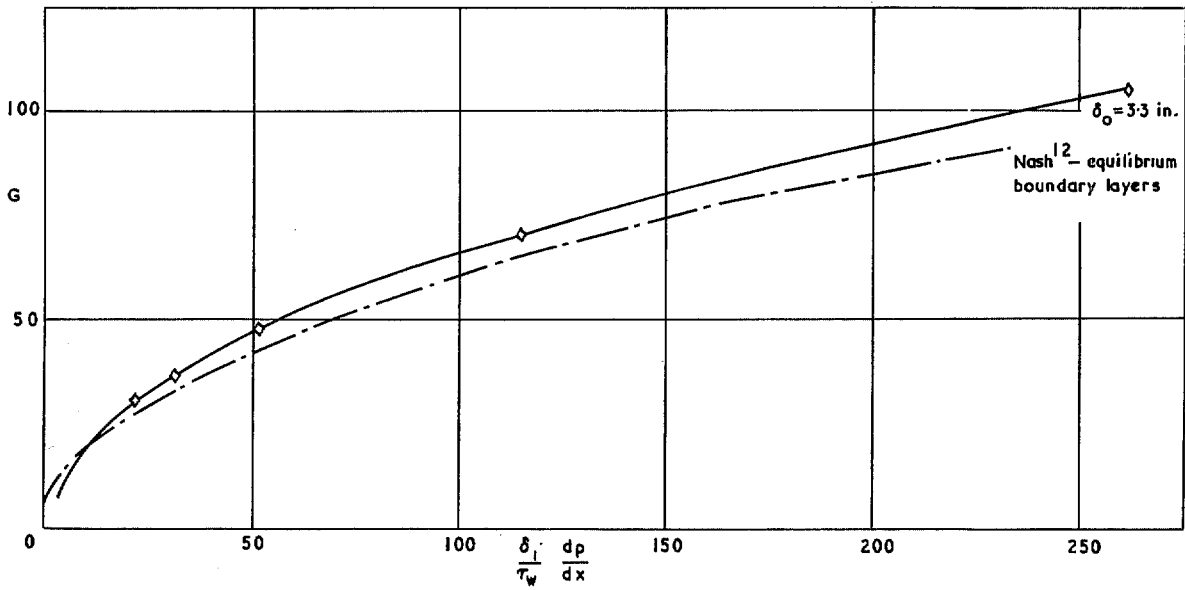


FIG. 15b. Large  $\frac{\delta_i}{\tau_w} \frac{dp}{dx}$

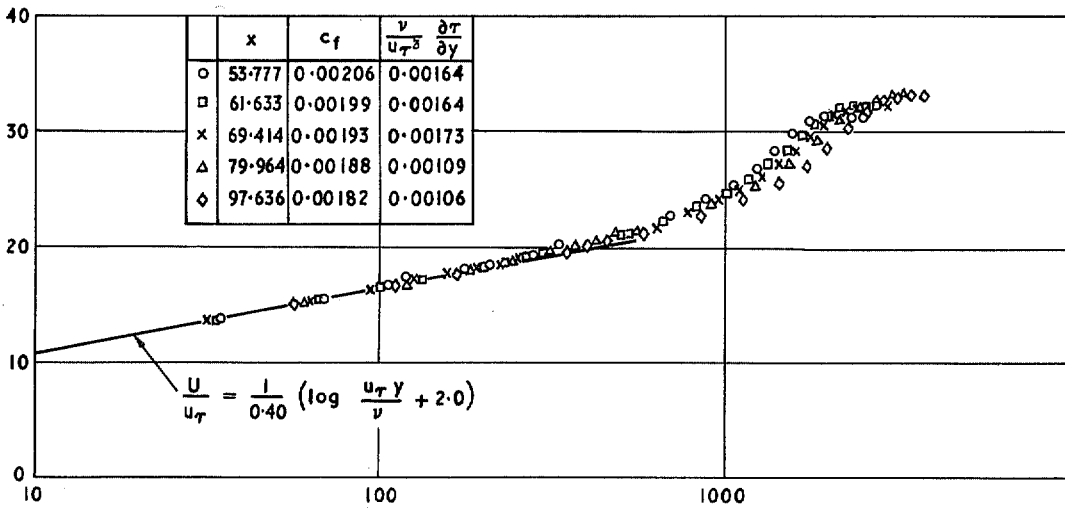


FIG. 16a. Calculated velocity profiles – logarithmic plot. (a)  $\delta_0 = 0.6$  in.

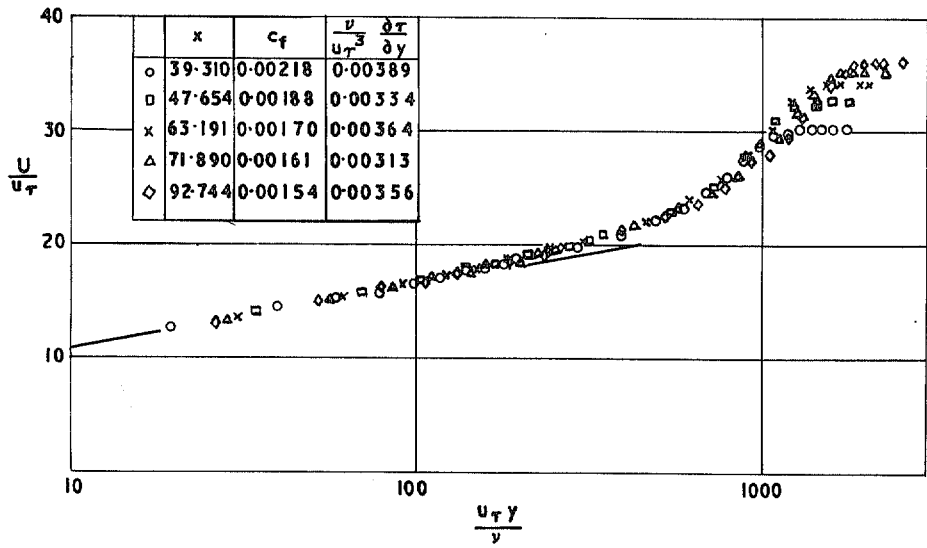


FIG. 16b.  $\delta_0 = 1.3$  in.

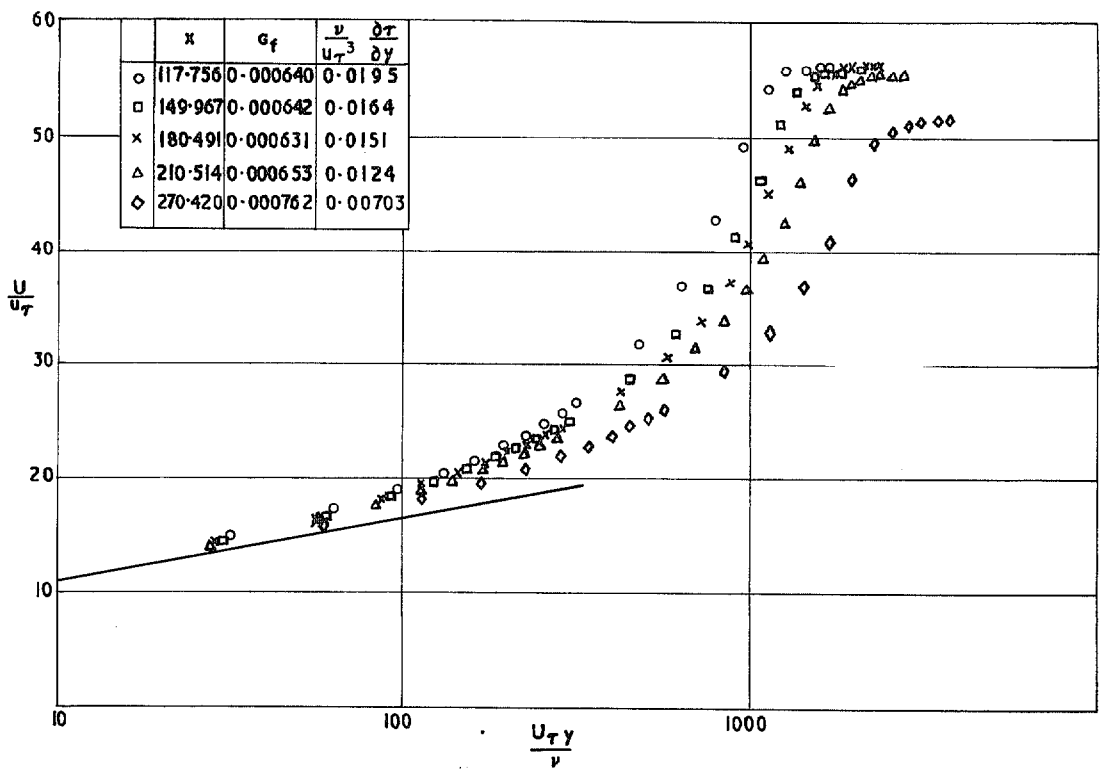


FIG. 16c.  $\delta = 2.6$  in.

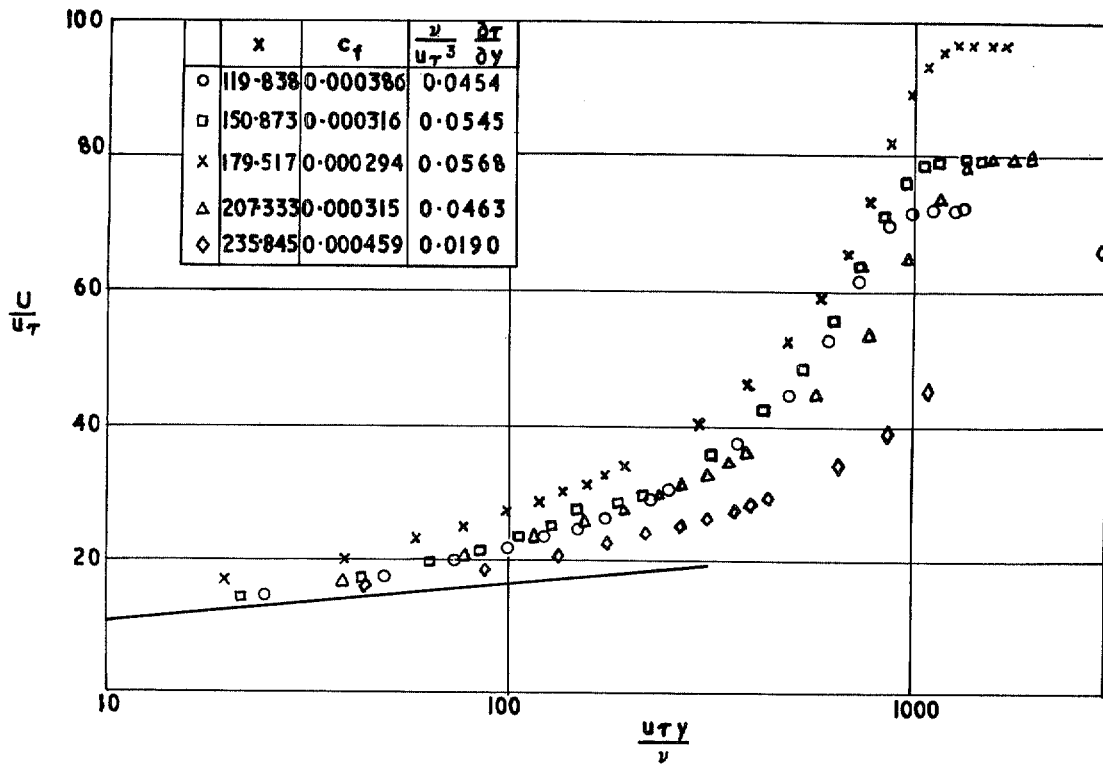


FIG. 16d.  $\delta_0 = 3.0$  in.

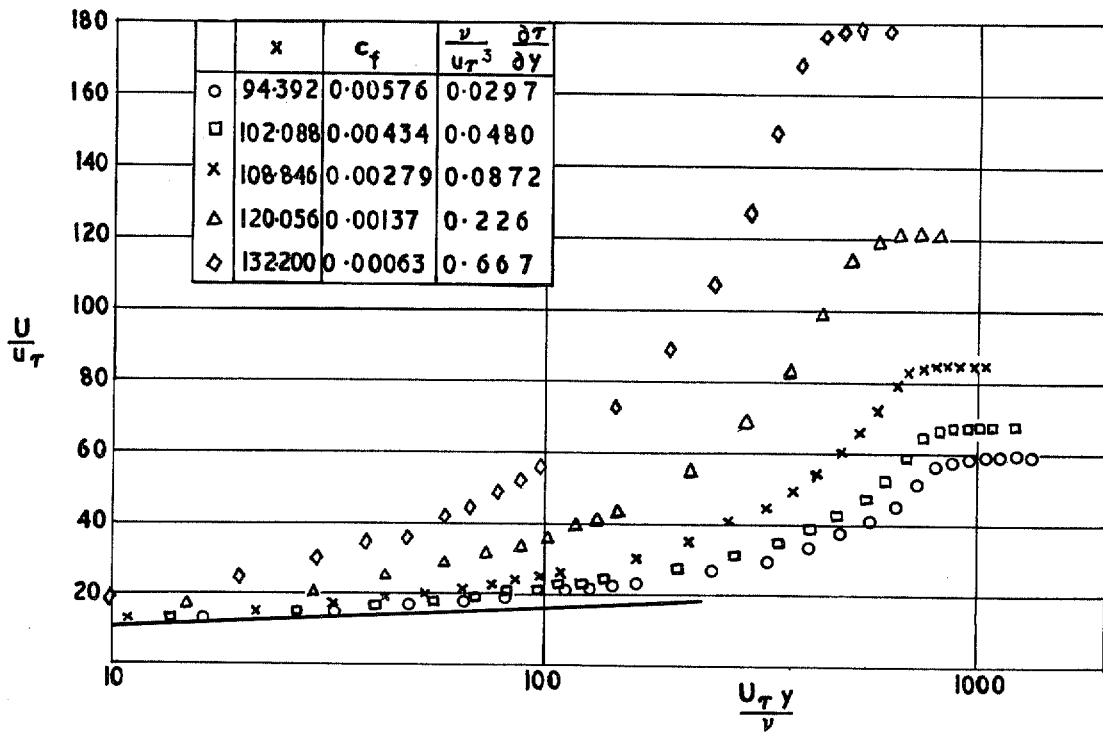


FIG. 16e.  $\delta_0 = 3.33$  in.

© *Crown copyright* 1969

Published by  
HER MAJESTY'S STATIONERY OFFICE

To be purchased from  
49 High Holborn, London w.c.1  
13A Castle Street, Edinburgh 2  
109 St. Mary Street, Cardiff CF1 1JW  
Brazennose Street, Manchester M60 8AS  
50 Fairfax Street, Bristol BS1 3DE  
258 Broad Street, Birmingham 1  
7 Linenhall Street, Belfast BT2 8AY  
or through any bookseller